UNIVERSIDADE DA BEIRA INTERIOR
Ciências

Understanding ion-exchange adsorption mechanism under overloaded conditions

Gonçalo Fradique Lopes da Silva

Dissertação para obtenção do Grau de Mestre em
Bioquímica
(2º ciclo de estudos)

Orientador: Prof. Doutora Ana Cristina Mendes Dias Cabral

Covilhã, Junho de 2013

Ao João, mãe, avós, tios

e Andreia

Acknowledgments

I would to thank to Professor Cristina Cabral for the best supervision and guidance during this last year. It was because of her efforts that this work went through. She was always available to help and teach me whenever I needed to.

Filipa, Patrícia, João and Chico created the perfect working environment in our lab. They were part of this. To Chico, a special thank for all his friendship.

To the rest of the friends and colleagues in the Investigation Centre I thank the support and the nicest coffee-breaks ever.

To my dear friends and family, who were always there to support me and never stop believing, I wish all the best.

A very special thank to Herr Egbert Müller because of his kind welcoming in TOSOH Bioscience. It was because of his prompt availability and help that part of this project went forward.

Last but not least, to Andreia, for her love and beliefs.

Resumo

A Cromatografia de Troca Iónica (IEC) é uma técnica muito eficaz e bastante usada na indústria biotecnológica. O maior desafio que qualquer técnica cromatográfica é prever o mecanismo the adsorção de biomoléculas nas resinas. Com esta investigação tentou-se examinar a complexidade da adsorção de proteínas em suportes de troca iónica. Os resultados de microcalorimetria de fluxo (FMC) e as isotérmicas permetiram ilustrar os processos de adsorção de lisozima em carboximetil celulose (CMC) tanto na ausência como na presença de sal (NaCl 50mM) a pH 5. Os resultados de FMC mostraram que sob todas as condições utilizadas a adsorção é, tal como esperado em troca iónica, conduzido entalpicamente. Uma correlação direta entre estes resultados e as isotérmicas pode ser estabelecida. Em condições lineares de proteína, a adsorção de lisozima ocorre na mesma extensão independentemente da concentração de sal. Contudo, quando se atinge o ponto de inclinação da isotérmica, a reorientação de lisozima na presença de sal parece ser o mecanismo condutor para uma posterior adsorção. Em condições de sobressaturação, na presença de sal, com o aumento da concentração de superfície e como uma nova camada de moléculas de proteínas é formada, é esperado um decréscimo do calor total da interacção, consistente com um equilíbrio energético a favor da formação dessa nova camada. Foram também realizados estudos em FMC e isotérmicas de adsorção de Albumina de Soro Bovino (BSA) em Toyopearl® GigaCap Q-650M. Estes resultados mostraram que o calor global desta interação é altamente exotérmico. É aparente que a alteração de conformação de BSA leva a uma adsorção secundária à superfície. Ainda, a altas concentrações de proteína à superfícies, podem ocorrer elevadas interações repulsivas. Estes resultados confirmam que a FMC é uma técnica eficiente que permite ilustra os mecanismos de adsorção de proteínas em IEC.

Palavras-chave

Cromatografia de Troca Iónica; Microcalorimetria de fluxo; Isotérmicas; Adsorção; Carboximetil celulose; GigaCap Q-650M; Lisozima; Albumina de Soro Bovino.

Resumo alargado

A Cromatografia de Troca Iónica (IEC) é uma técnica de purificação bastante popular e muito usada na indústria biotecnológica. A sua popularidade deve-se às suaves condições de trabalho usadas que permitem manter a estabilidade e atividade do produto desejado durante o processo. Esta técnica baseia a separação de biomoléculas na atração eletrostática entre o suporte cromatográfico carregado eletricamente e o produto com carga oposta. Apesar de bem descrita, ainda muito há por saber sobre este tipo de cromatografia, nomeadamente sobre os mecanismos subjacentes à adsorção de proteínas a uma resina de troca iónica.

Essenciais a todos o processo de purificação são os custos associados. Estes podem ser reduzidos aumentando o rendimento do processo (quantidade de produto obtida por unidade de tempo). Por estas razões, é imperativo aumentar a quantidade de produto inicial, trabalhando para isso em condições de sobressaturação.

Também associado a uma purificação mais eficiente está o tipo de suporte utilizado. Quanto maior for a afinidade do produto desejado para o suporte, maior será a o rendimento final do processo. Há então vários tipos de resinas disponíveis no mercado. Neste trabalho foram usadas duas resinas de troca iónica forte (carboximetil celulose (CMC) e Toyopearl GigaCap Q-650M) e uma de troca iónica fraca (Toyopearl DEAE-650M), sendo que o GigaCap tem alterações poliméricas na sua matriz de modo a conseguir uma maior área de contacto com a proteína.

Esta dissertação tem por objetivo melhorar a compreensão dos mecanismos de adsorção de proteínas modelo (lisozima e albumina de soro bovino (BSA)) a suportes de troca iónica comerciais em condições de linearidade e de sobressaturação de proteína considerando o efeito da força iónica.

A microcalorimetria de fluxo é uma técnica que permite a deteção de pequenas alterações de calor dentro de um sistema cromatográfico. Ora, como os processos de adsorção em troca iónica são, à partida, processos exotérmicos, existe uma transferência de energia associada, a microcalorimetria pode assim ser usada para ajudar a compreender os mecanismos subjacentes a este tipo de adsorção.

Foi observada uma correlação direta entre os resultados de microcalorimetria e os das isotérmicas de adsorção, tanto para os testes de troca catiónica (lisozima-CMC) como para os de troca aniónica (BSA-GigaCap Q-650M).

Para os ensaios com lisozima, foi verificado que em condições lineares de concentração de equilíbrio de proteína, os processos de calor exotérmico envolvidos dão-se na mesma extensão tanto na presença como na ausência de sal. Isto parece indicar que pelo facto de o

suporte cromatográfico ainda não estar saturado, a adsorção de proteína à superfície dá-se livremente.

No entanto, na presença de sal, quando a resina começa a ficar saturada, nota-se um aumento do calor endotérmico, o que pode indicar um aumento de reorientação das moléculas de lisozima de modo a permitiradsorção de mais moléculas. Isto parece ser confirmado com a elevada libertação de energia que também ocorre nessas condições de sal e de concentração de proteína à superfície.

Em condições de sobressaturação, é observado que o aumento da concentração de superfície leva a uma diminuição do calor envolvido em todo o processo. Isto é expectável, tendo em conta que a energia que as moléculas necessitam para se reorientarem, é gasta em adsorção, estabelecendo-se assim um equilíbrio na formação de uma nova camada de moléculas à superfície. Também a formação de multicamada de moléculas de proteínas a concentrações de equilíbrio superiores pode ser possível.

Já os ensaios de BSA com a resina oferecida pela TOSOH Bioscience, resultaram em reações altamente exotérmicas, havendo a presença de três picos desse tipo de calor. A intensidade do primeiro deles diminui à medida que a concentração de BSA à superfície da resina aumenta. Como estes testes foram efetuados na ausência de sal, isto pode ser justificado com o aumento de repulsão entre moléculas adsorvidas que advém do aumento de concentração à superfície.

A intensidade do segundo pico exotérmico também diminui com o aumento da concentração de superfície. Ora, como a concentrações baixas as interações proteína-suporte são mais fortes, isto leva a maiores alterações de conformação de proteína, que permite uma adsorção secundária.

O último pico que é exotérmico a baixas concentrações, torna-se endotérmico às concentrações de superfícies mais elevadas, podendo indicar elevada repulsão entre as moléculas adsorvidas.

Todos estes resultados confirmam que, para uma visão mais consistente do mecanismo de interação de troca iónica, a utilização da microcalorimetria de fluxo mostra-se de grande interesse no estudo sistemático dos diferentes suportes comerciais disponíveis.

Abstract

Ion-exchange chromatography (IEC) is a powerful and widely used separation technique in the biotechnological industry. The greatest challenge of any chromatographic technique is predicting the adsorptive behaviour of biomolecules onto the chromatography resin. This investigation attempts to examine the complexity of protein adsorption onto ion-exchangers and the role of nonspecific effects in the establishment of the adsorptive process. Flow microcalorimetry (FMC) and adsorption isotherms measurements were used to illustrate lysozyme adsorption mechanism on carboxymethyl cellulose (CMC) at both absence and presence of salt (NaCl 50mM) at pH 5. FMC results show that under all the studied conditions the adsorptive process is, as expected in ion exchange, enthalpy driven. Direct correlation between microcalorimetry data and isotherm measurements is observed. Under linear protein concentrations, protein adsorption occurs in the same extension regardless salt concentration. However, when isotherm levelling point is reached, lysozyme reorientation in the presence of salt seems to be the leading mechanism to further adsorption. Under overloaded conditions in the presence of salt, with increasing surface concentration, as a new layer of protein molecules is formed, an expected decrease in the net heat of adsorption is observed, consistent with an energetic equilibrium towards the formation of the new layer. FMC experiments and isotherm measurements were also performed for Bovine Serum Albumin (BSA) adsorption onto Toyopearl® GigaCap Q-650M. The results showed a high overall exothermic process. Secondary adsorption of BSA to the surface, resulting from its alteration of conformation seems to be present. Also, at high protein surface concentrations, high repulsive interactions may occur. All these results confirm that FMC is a powerful technique to illustrate protein adsorption mechanisms in ion-exchange.

Work supported by FCT (Portuguese Foundation for Science and Technology), project number FCOMP-01-0124-FEDER-014750 (Ref. FCT PTDC/EBB-BIO/113576/2009) and NSF (American National Science Foundation) NSF – 1246932 (award issued by CBET division of NSF)

Keywords

Ion-exchange chromatography; Flow microcalorimetry; Isotherms; Adsorption; Carboxymethyl cellulose; GigaCap Q-650M; Lysozyme; Bovine Serum Albumin.

Índice

Lista de Acrónimos

AAI	Available Area Isotherm
BSA	Bovine Serum Albumin
CMC	Carboxymethyl cellulose
DCB	Dynamic Binding Capacity
FMC	Flow Microcalorimetry
HIC	Hydrophobic Interaction Chromatography
IEC	Ion-Exchange Chromatography
ITC	Isotherm Titration Calorimetry
Lys	Lysozyme
NISS	Non-ideal Surface Solution
SDM	Stoichiometric Displacement Model
SMA	Steric Mass Action
ΔG	Gibbs free energy variation

Chapter 1 – Introduction

1.1 – Liquid chromatography for biomolecules

Chromatography is a powerful technique that makes part of the downstream process for separation and purification of biomolecules. This purification technique is based on a retardation of molecules as the solvent progresses through a stationary phase. The stationary phase, with certain characteristics, is packed in a column and the mobile phase works as an eluent that carries the sample to be purified. Biomolecules are purified through a stationary phase according to a given property, such as size, charge, hydrophobicity or biospecific interaction [1]

In this work, we intend to understand the adsorption mechanisms in ion exchange chromatography (IEC) with a special focus on overloaded conditions.

Ion-exchange mechanism for preparative separation has been widely used in the pharmaceutical industry [2–8]. The popularity of this technique is due to its simple and easy to use methodology. Also, it is used under mild pH, temperature and salt conditions, allowing preserving the biological activity of the biomolecules during the process [3–9]. Another advantage of IEC is the usage of aqueous buffers and hydrophilic surfaces [9].

One efficient way to increase the overall throughput in chromatography is to increase the dynamic binding capacity of the resins [10]. Ion exchange resins have dynamic binding capacities higher than those of the other chromatographic modes. In this way, it is the most chosen method for the capture and concentration step [11].

1.2 – Goal of study

Essential to the overall process are the costs associated with the downstream process, which can be reduced by increasing the overall throughput (product per time unit) [10]. Due to these economic reasons, chromatography should be run under overloaded conditions despite being much more complex to operate than the linear mode [12–14]. Also, running chromatography under the overloaded mode results in undesirable non-specific interactions.

Unlike analytical operations which have suitable linear equilibrium descriptions, there is still lacking an appropriate model to describe non-linear equilibrium [13,14]. This region of the adsorption isotherm is important for overloaded chromatography, however due to associated

non-ideal interactions of protein adsorption and desorption, a reliable separation mechanism could not be predicted yet [2]. Since the free energy contributions of the underlying processes cannot be properly estimated, the design and optimisation of preparative chromatography systems has not been possible [15].

Chapter 2 – Background and research objectives

2.1 – Ion-exchange liquid chromatography

Ion-exchange chromatography is based on electrostatic interactions between the product and the oppositely charged groups of the stationary phase. In first place, there is an adsorption step, in which the desired product binds to the adsorbent and the rest of the loaded mixture is washed away as the mobile phase flows through. After that, the mobile phase conditions are changed (increasing salt concentration or changing the solution pH) and the target molecule is eluted [1,16].

IEC has to be carried at a pH within a range between the isoelectric point (pI)- pH at which the protein is uncharged- of the protein and the pKa of the packed resin. Considering this, this type of chromatography can be either cation- or anion-exchange. In cation exchange chromatography the desired molecule is positively charged while the adsorbent is negatively charged, so one has to work at a pH lower than the pI. On the other hand, anion exchangers bound proteins with negative net charge; therefore the pH should be higher than protein's isoelectric point. However, since proteins are relatively unstable, the pH range at which liquid chromatography should be carried out has to consider protein stability [16]. Furthermore, it should be also taken into account the conditions of adsorption and elution to minimise non-specific interactions [10].

As it can be seen in Figure 2.1.1, that shows a schematic representation of ion exchange chromatography, molecules that have more affinity (higher density of opposite charges) to the resin stay in the column more time than the ones that do not. Elution may be carried with high salt concentrations, where the counter ions present bind to solute and adsorbent surface in order to decrease one's attraction to the other.

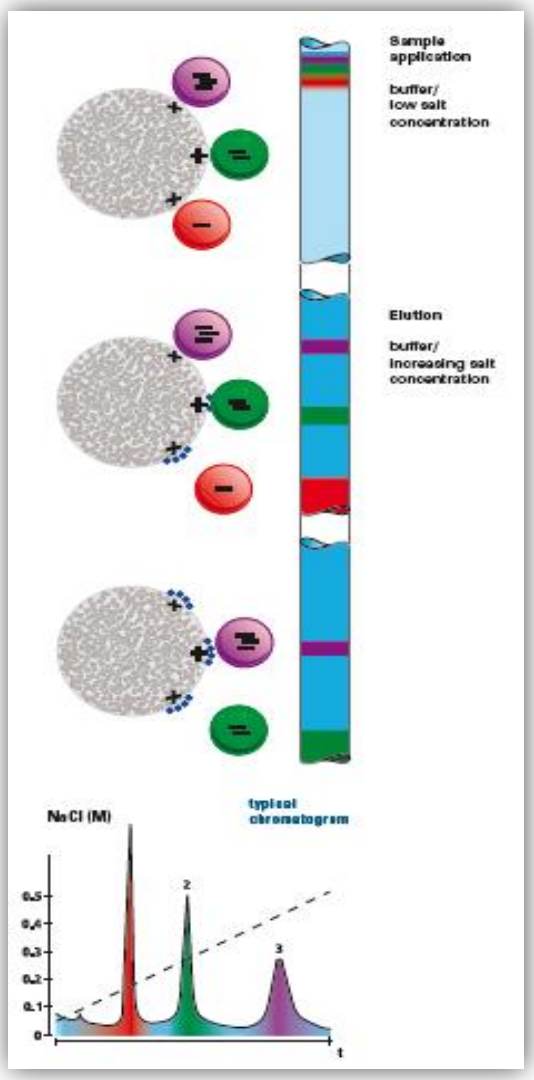

Figure 2.1.1 – Ion exchange chromatography illustrative representation adapted from [17].

The stationary phase has to be chosen accordingly to the research goal. In order to increase productivity, working under high flow rates is almost mandatory [18]. Therefore, a balance between high binding capacity, rapid kinetics and mechanical strength has to be found [18]. In addition, ion exchangers must be stable enough to resist acidic or caustic washing [16].

In this study three different ion exchangers were used: carboxymethyl cellulose (CMC), a strong cation exchanger with a small ligand, bought from Whatman Ltd.; Toyopearl® DEAE-650M, a weak anion exchanger and Toyopearl® GigaCap Q-650M, a strong cation exchanger with a certain degree of ligand grafting. The last two were offered by TOSOH Bioscience.

2.2 - Column characterisation

Ion exchange is a chromatographic operation technique in which reversible adsorption between two oppositely charged surfaces (solute molecules and chromatographic resin) takes place. The purification of the target molecules depends on the difference in the attraction strength to the adsorbent between the desired product and other solutes present. Therefore, every ion exchanger has a specific capacity for a different solute according to its charge and ionic strength of the media [19,20].

Another factor that affects protein binding capacity by an adsorbent is the mass transfer associated to the chromatographic process [21]. For this reason, the dynamic binding capacity (DBC) of a resin to a specific protein is limited, contrary to its ideal and theoretical (static) binding capacity. Associated with mass transfer of proteins are: pore diffusion, surface diffusion, film diffusion and interaction kinetics [10,22].

Large-scale preparative chromatography has different critical factors compared with analytical chromatography, such as capacity, recovery and throughput [23]. One way to increase the overall throughput is to operate under a high flow rate [23]. However, according to Van Deemter equation [24] there is an optimum linear velocity (μ) that minimises flow diffusion (A), particle longitudinal diffusion (B) and mass transfer phenomena (C).

$$\mathrm{HETP} = A + \frac{B}{\mu} + C.\mu \qquad (1)$$

All things considered, static binding capacities represent an upper bound to the dynamic ones, which simulate actual chromatography conditions.

2.2.1 - Static binding capacity

Protein adsorption and adsorbent's capacity are dependent not only on the physical chemistry properties of both species but also on protein equilibrium concentration [25]. One can say that binding capacity increases linearly with protein equilibrium concentration until a certain point. When adsorbent's binding sites start to become saturated with protein, adsorption of more molecules is limited [25]. Bellot and Condoret stated that molecules are adsorbed on a fixed number of well-located sites, which accept only one molecule, and are organised as monolayers; all sites are energetically equivalent and no interaction between adsorbed molecules occurs [25]. However, when working with biomolecules, adsorption mechanisms are

not that simple. In this way, several empirical and semi-empirical equilibrium models have been used to try to understand protein adsorption [15].

The Langmuir isotherm is a simple theoretical model used to describe adsorption of one component. It states that the molecules are adsorbed on a limited number of sites, which accepts only one molecule. Also, every adsorption site is energetically equivalent and there is no interaction between adsorbed molecules [26]. At low concentrations, the molecules are well distributed at the adsorbent surface, resulting in a linear shaped curve between adsorbed amounts and mobile phase concentration. At higher concentrations, the adsorption sites become saturated, leading to a curvature of the isotherm to an asymptote [25]. It does not take into account solute-solute interactions [25] and does not consider the sterical arrangement of the ligands as well [10]. Nevertheless, although complex systems cannot be properly described by this model, Langmuir isotherm has been long used to describe equilibrium regarding protein adsorption [25], where K is equilibrium constant, q_m the total binding capacity of the resin, C_{eq} is protein concentration at equilibrium and q_{eq} represents the adsorbed amounts at equilibrium:

$$q_{eq} = \frac{(q_m * \mathrm{K} * C_{eq})}{(1 + \mathrm{K} * C_{eq})} \qquad (2)$$

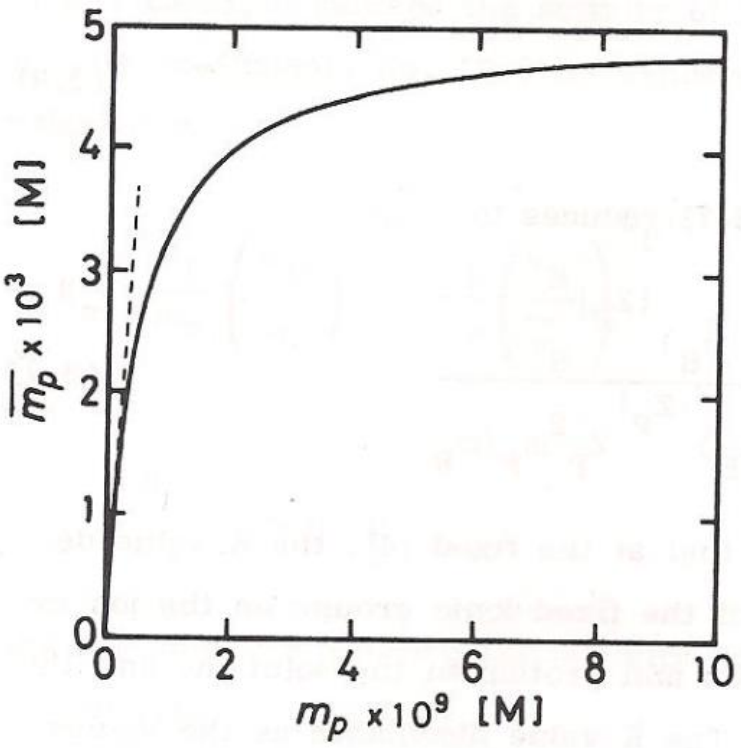

Figure 2.2.1.1 – Langmuir isotherm representation adapted from [16].

Usually, in order to characterise competitive non-linear chromatographic systems, multicomponent Langmuir isotherms have been used [27,28]. Despite being reliable to predict the elution times and band shapes of the different components [25,28] multi-component isotherms still do not have a proper description of adsorption equilibrium [29,30]

Other models to explain equilibrium have been used. Kopacievicz et al. [31] and then Rounds and Regnier [32] described the stoichiometric displacement model (SDM). This model describes protein retention in linear IEC and assumes that ion exchange is the only adsorption mechanism. Since SDM states that the entire ion exchange capacity is available to protein adsorption, it is an accurate model for low protein concentrations. Despite not being as reliable for high protein loadings [13,14], it was later applied and developed for overloaded conditions [33,34].

Many scientists, for instance Kopacievicz and co-workers [35] and Thrash and Pinto [9] have also shown that not only electrostatic interactions exist in IEC. They concluded that haemoglobin was not able to elute from an anion-exchanger at high ionic strength, even though it could be performed with a non-polar solvent. So, in spite of being a process mainly based on interactions of opposite charge materials, ion exchange chromatography, it may also have some hydrophobic and non-specific interactions involved [36].

In order to model non-linear elution of proteins in IEC, Brooks and Cramer proposed in 1992 [37] the Steric Mass Action (SMA) model. This model predicts the salt dependence of protein adsorption and the steric shielding occurring under overloaded conditions [28]. It proposes that the steric hindrance is related to the protein surface concentration [13,28]. Gallant and co-workers have focused on two important effects in preparative chromatography: the salt dependence of protein binding and the adsorption in non-linear conditions.

These mass-action models for the estimation of protein isotherms describe adsorption as a stoichiometric exchange of ions between the resin surface and the protein. In this way, such models do not describe major non-ideal effects associated with protein adsorption, or when they do is in a thermodynamically inconsistent way [15]. Li and Pinto [38] proposed the non-ideal surface solution (NISS), which, based on SDM, described non-ideal effects of protein adsorption in a thermodynamically manner. In the NISS model the adsorbed phase is characterised as a non-ideal surface solution that is controlled by adsorbed protein interactions in the neighbourhood. The liquid phase is assumed to be a non-ideal bulk liquid controlled by the interactions between modulator ions.

In order to check which effects actually limit protein adsorption, Raje and Pinto [13] combined SMA and NISS. It was concluded that there is still left to understand which of the two effects (steric hindrance or non-ideal surface interactions) control adsorption under overloaded conditions. Later, they showed that the heat of adsorption of chloride ions in the surface of an ion exchanger is independent of the surface coverage, indicating that the already adsorbed ions do not affect the adsorption of the subsequent ions [14]. However,

when it came to protein adsorption, the results showed that there is dependence on the surface coverage in this phenomenon. The heat of adsorption decreased with the increasing of surface coverage, suggesting repulsive interactions between adsorbed proteins.

All things considered from all the models mentioned, it can be summarised that: SDM does not consider non-ideal effects under overloaded conditions; SMA consider non-ideal effects, but, apart from steric hindrance, assume other negligible; NISS consider non-ideal effects, such as repulsion between like charge proteins, but neglect steric hindrance.

Another type of protein isotherm model is the colloidal method. Oberholzer and Lenhoff [39] expanded this method even more and described protein isotherms under overloaded conditions. They incorporated the average lateral interactions into the isotherm as a correction to linear adsorption, considering them as a function of surface coverage. Isotherm prediction depends on the balance between protein-surface attraction and adsorbate-adsorbate repulsion. It is now known that these two phenomena can be decoupled [39]. Nevertheless, when these repulsion mechanisms are associated with high affinity for the adsorbent surface, the extent of the adsorption process may be limited.

Another isotherm prediction model developed was the Available Area Isotherm (AAI) [40]. While the previous models were developed for adsorption of small molecules, the AAI, suggested by Bosma and Wesselingh, accounts for geometrical exclusion due to already adsorbed proteins. This model fits for protein adsorption both in IEC and HIC. It has a better thermodynamic foundation since instead of the isotherm being determined by the charge of the proteins, it is determined by the effect of large size proteins accompanied by geometrical exclusion.

2.2.2 – Dynamic binding capacity

The dynamic binding capacity of a chromatographic column characterise the performance of a packed column with a given adsorbent. It is often defined as the amount of protein bound to the resin under the running conditions when the effluent concentration reaches a specific breakthrough of the protein feed concentration [41].

The dynamic binding capacity of a chromatography column can be expressed according to the following equation:

$$DBC_{10\%} = \frac{C_f * \mathrm{Q} * t_{10\%}}{V_0} = \frac{C_f * V_{10\%}}{V_0} \qquad (3)$$

where the Q is the volumetric flow rate of the load, the t10% and the V10% are the breakthrough time and volume at which the effluent reaches 10% of the feed concentration (C_f), respectively [41].

The DBC is a characteristic of the ion-exchange support and is depended on the residence time [41] and, therefore, on the flow through. In addition, the mobile phase conditions, such as conductivity and pH, affect the binding capacity of the resin [42–44]. It is known that the capacity of an ion-exchange chromatography support to bind a given protein decreases when protein net charge decreases and buffer conductivity increases [37].

However, a second mechanism is presented by Harinarayan [43], in this case, the complete opposite occurs; the binding capacity of a given matrix unexpectedly increases as the conductivity increases and the protein net charge decreases. This can be explained by an exclusion mechanism, which predicts protein binding to the outer surface of the resin bead. In this way, by charge repulsion and steric exclusion, additional protein molecules transportation through the pore is reduced [44]. So, by lowering the protein charge or raising the salt concentration (increasing conductivity), the charge repulsion effect between the protein molecules lowers, allowing higher dynamic binding capacities [43].

Furthermore, the DBC is a function of the resin itself; some of its characteristics, like the pore size, also have influence on the binding capacity of a column. Theoretically, in a same sized particle, the smaller the pore size the higher the surface area. Also, as the pore size increases, the access to the internal surface area also does ([10,11]). The binding capacity of a protein increases as the pore becomes larger until its maximal access to the internal surface area. Nevertheless, since the absolute surface area decreases with the pore size enlargement, there is a point of diminishing return and the protein binding capacity starts to diminish [11]. The pore size of a given support is influenced by the type of ligand attachment and architecture. Depending on this, the effective pore size of the resulting resin is smaller than the one of the initial bead [10,11]. According to Müller [21], both pore size optimisation and polymeric surface modification are further improvements in order to enhance mass transfer and therefore the DBC.

2.3 – Microcalorimetry as a tool to investigate surface phenomena

As it was previously described, working under overloaded conditions originates non-idealities during adsorption in chromatography [2]. Therefore, reliable and satisfactory isotherm prediction may not be that easy. Some empirical models, like Langmuir, are often used to fit experimental isotherm, even though it is a risky approach. Although IEC is commonly used, the underlying mechanisms that establish equilibrium in adsorption are not yet properly

described. The so far proposed models have shown some limitations because non-specific intermolecular interactions are not fully understood. In this way, considering all these points and to try to overcome the already mentioned difficulties, researchers have been focusing in calorimetry.

Equilibrium is dictated by the Gibbs free energy (ΔG), and overall ΔG depends on reaction enthalpy and entropy [9]. Protein adsorption can generate a small yet measurable thermal signal, which can help describing the adsorption mechanism [15,45,46], so reaction enthalpy can be measured with microcalorimetry. Thus, this technique can provide valuable insight about the underlying mechanisms of adsorption [9,12,47].

Isothermal titration calorimetry (ITC) is a calorimetric method that works under the batch mode. The measurement of heat exchange represents the energy associated to the whole adsorption process, including dilution heat, binding heat, energy required for desolvation, energy change after biomolecule rearrangement… However, information about the desorption process is not possible to obtain by this technique [48].

On the other hand, flow microcalorimetry (FMC) works under a specific flow rate. Therefore, heat measurements can be calculated for desorption, so that the level of reversibility can be determined according to both heat and mass transfer. The whole profile can give an overview on the kinetics of process adsorption and desorption. Also, by integrating the obtained values, energy change can be determined in order to the associated mass transfer [12,49,50].

Thermodynamically, adsorption in ion-exchange chromatography is expected to be exothermic, once there is release of energy when two surfaces with opposite charges approach each other. However, previous calorimetric studies [2,9,14,15,51,52], have shown that protein adsorption might be endothermic as well. Therefore, since the Gibbs free energy has to be negative for a favourable reaction, this process must be entropically driven. There are several non-specific effects that might be the source of endothermic interactions: repulsive interactions between adsorbed molecules; repulsive interactions between protein surface hydrophobic groups and adsorbent surface hydrophilic moieties; repulsive interactions between like charge groups on the protein surface and on the adsorbent surface; water release from adsorbent's and protein's surface; protein conformational changes; protein reorientation on the surface [14,52].

For ion-exchange chromatography it was then suggested that when enthalpy change was not favourable, water release due to hydrophobic interactions was the factor leading to an increase of entropy, as well as structural rearrangements and changes [53]. However, since some studies relate endothermic heat to expected sources, other to conformational changes [14,49,52,54], and some to water release [54,55] it is important to investigate the sources of endothermic behaviours.

Thrash et al [2] tried to understand the mechanisms underlying IEC under the overloaded mode. For that, they studied the interaction of Bovine Serum Albumin (BSA) with an anion-

exchanger with FMC under both, linear and non-linear loading conditions. The isotherm results showed a typical Langmuir curve with higher adsorption capacities at lower ionic strengths. It was also concluded that there is more than electrostatic interactions controlling this process. Water release seemed to be high enough to overcome unfavourable enthalpy change at 25°C. However, at 37°C the free energy reduction resulting from water-release-associated entropy increase was not great enough to overcome unfavourable enthalpic interactions. Therefore, higher temperatures appear to be associated with structural rearrangements, contributing to drive adsorption through an entropically way [2]. On another study [15] concerning the adsorption of BSA and ovalbumin onto an anion-exchange sorbent, the same authors, demonstrated that electrostatic repulsive interactions between adsorbed molecules appeared to be a larger contributor to endothermic heats of adsorption than surface dehydration or solution non-idealities. They also found that the presence of mobile phase cations can reduce the magnitude of endothermic adsorption heats by screening repulsive interactions between adsorbed molecules. Although water release was not found to be a major contributor to endothermic adsorption heats, they considered it a contributor to the entropic driving force associated with the adsorption of BSA.

In 2006, Thrash *et al*. used the colloidal model, represented in Figure 3, in combination with heat of adsorption studies and concluded that protein capacity in IEC is strongly limited by repulsive interactions between adsorbed proteins [9,15].

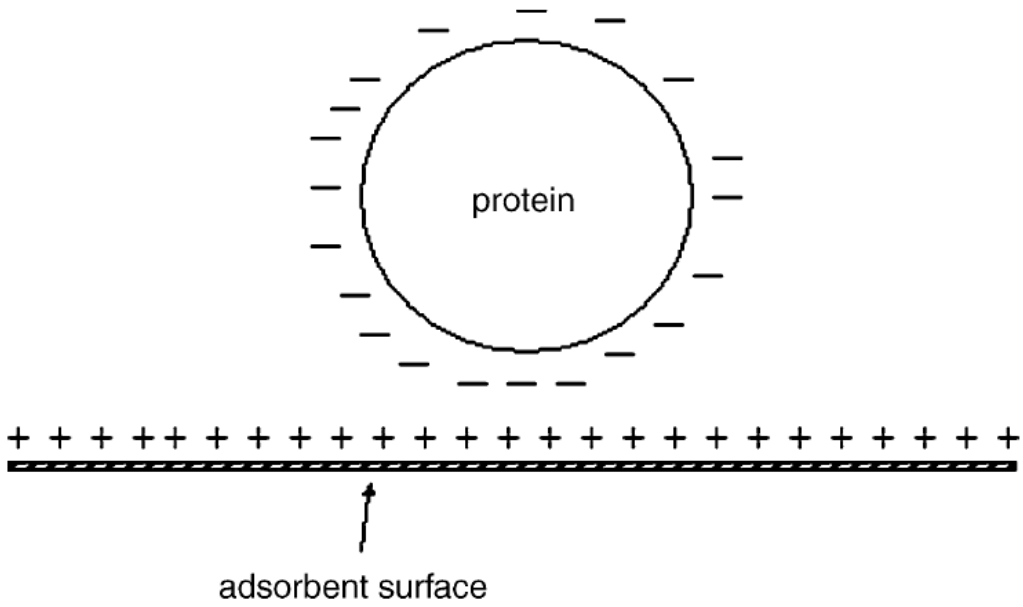

Figure 2.3.1 – Schematic representation of colloidal approach for modelling protein adsorption on an ion exchanger, adapted from [15].

The protein adsorption heat was endothermic for all the experiments, meaning that it was the increase of entropy from water release that made the adsorption energetically favourable. In addition, it was shown that the type of the ionic buffer used affects the repulsive interaction between adsorbed proteins and also the release of water [15].

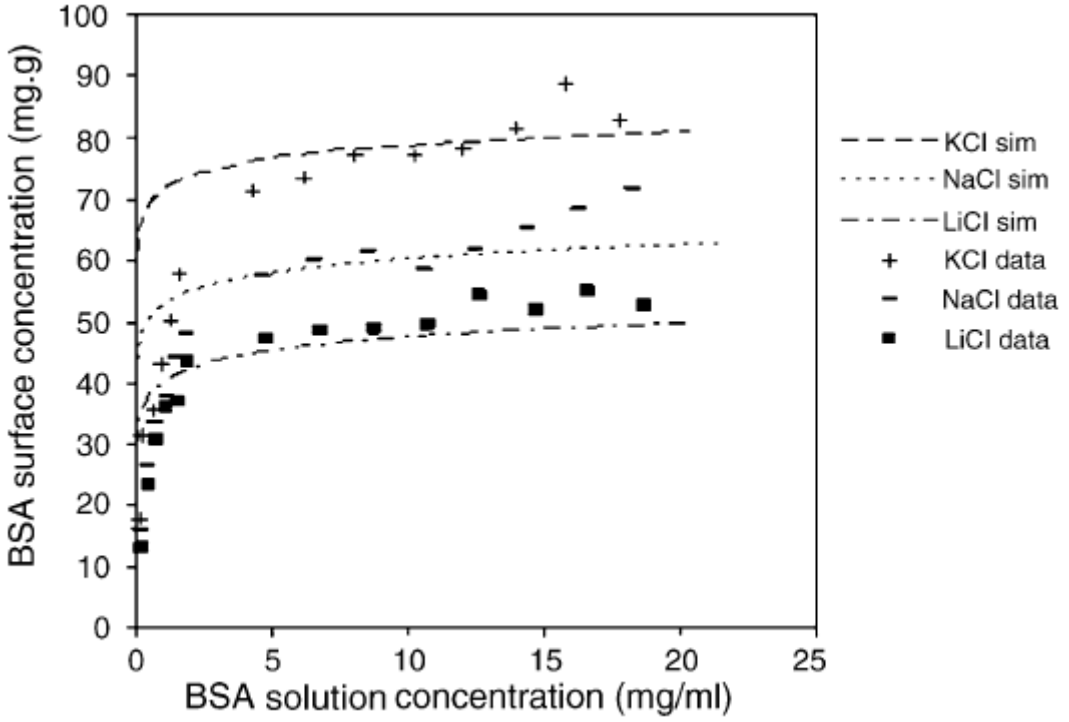

Figure 2.3.2 – Comparison of simulated and experimental isotherms for BSA in the presence of different salts (298K; pH 6,2; 100mM of each salt), adapted from [15].

Similar studies have been done in hydrophobic interaction chromatography (HIC) a process where water molecules are released from protein and adsorbent's surface due to the presence of salt which leads to a reduction of total hydrophobic area [56,57], allowing protein interaction with the surface. Dias-Cabral et al [49,50] stated that this water release increases the entropy of the system without actually changing significantly its enthalpy, suggesting adsorption as an entropically driven process in HIC [58,59], contrary to IEC. It was also concluded that under overloaded conditions adsorption is enthalpically driven instead. This was due to not only attractive interactions between adsorbed proteins at high ionic strength but also due to conformational change of these proteins during adsorption.

From the exposed before it seems that different segments of the literature have different explanations for the heat exchange during an ion-exchange interaction. The true, is that all of them are correct because it system has its specificities. So, for a more consistent overview

of the mechanism of interaction, flow microcalorimetry could be of great help in a systematic study of ion-exchange chromatography.

2.4 – Research objectives

As mentioned, it is well recognized that ion-exchange chromatography is a powerful technique for the separation and purification of biomolecules on a large process scale, resulting from the superimposition of different effects: fluid dynamics, mass transfer phenomena and equilibrium thermodynamics. It is imperative, for economic reasons, to run the chromatographic process in the overloaded mode. However, operation in the overloaded mode is considerably more complex than linear chromatography, and suitable models do not exist. Consequently, the prediction of separation behavior is generally unreliable. This is a major impediment in the design and implementation of scaled-up units. There is, therefore, considerable practical interest in developing a better understanding of the mechanisms underlying non-linear chromatography of biomolecules. Thus the specific goals for this project will be the investigation in IEC of the effect of salt and support type on the adsorption mechanism under linear and overloaded conditions. Two different types of adsorbents (cation and anion-exchange) will be used.

Flow microcalorimetry will be extensively used to study the non-ideal interactions under overloaded conditions, as previous studies have underscored the importance of calorimetry as a means to investigate surface phenomena. Also, adsorption isotherms and dynamic binding capacity data will be obtained at different operation conditions to characterise IEC adsorption mechanism under non-linear conditions.

This work will be done partly in Health Sciences Investigation Centre of Universidade da Beira Interior (CICS-UBI), Covilhã, Portugal (FMC studies and adsorption isotherm measurements) and in TOSOH Bioscience GmbH, Stuttgart, Germany (DBC studies and adsorption isotherms).

Chapter 3 – Experimental

3.1 – Adsorption isotherms

Lysozyme (Sigma-Aldrich) solutions were prepared in 20mM of piperazine (Mw = 86g/mol) buffer at pH 5 both without and with 50mM of sodium chloride (NaCl, Mw = 58,44g/mol). Carboxymethyl cellulose (CMC), bought to Whatman Company, was weighted into individual test tubes and then transferred with 1mL of protein solution to a multi-well plate. The plates were sealed with parafilm and were left to shake for 24h at 230rpm and 21,5°C. After equilibrium was reached, the slurry was transferred to Eppendorf tubes and left to settle for 30 minutes. The supernatant was then removed with a syringe and the absorbance of every solution was measured at 280nm with a UV spectrophotometer. In order to know the amount of protein bound to the adsorbent a mass balance was applied. The isotherm plot was done with lysozyme surface concentration against protein equilibrium liquid concentration.

The commercial resins kindly offered by TOSOH Bioscience, Toyopearl DEAE-650M and Toyopearl Gigacap-Q, were suspended in deionised water in a 50/50 mixture. BSA (Sigma-Aldrich) solutions with different concentrations were prepared in in 20mM of tris-HCl buffer at different salt conditions (0, 50mM and 100mM NaCl) and different pH (pH 8 for DEAE-650mM and pH 9 for GigaCap-Q). Protein solutions were then transferred to Falcon tubes along with the slurry of resin. The ratio of this gel to the total solution volume was 1:100. Equilibrium was reached after 5 hours of shaking at 50rpm at room temperature. Then, the resin was left to settle and protein equilibrium concentration was measured with NanoDrop 2000c (Peqlab Biotechnologie GmbH, Erlanger). This part of the study was done in TOSOH Biosience laboratories, in Stuttgart, Germany.

3.2 – Dynamic binding capacities

The dynamic binding capacities were performed in ÄKTA systems (Purifier and Explorer) (GE-Healthcare, Uppsala, Sweden). The two anion exchangers, Toyopearl DEAE-650M and Toyopearl GigaCap-Q, were packed in a 0,63mL column (Ø = 6,6mm; h = 1,85cm) according to manufacturer instructions [60]. The acetone test was performed in order to check the packing. For each resin the DBC was determined with different BSA loadings prepared with tris-HCl buffer at 20mM at different pH (7,2, 8 and 9) and with different ionic strengths (0, 50mM and 100mM NaCl). DBCs were measured under a flow rate of 150cm/h at 10% breakthrough. In first place, a specific protein concentration is loaded through the bypass to

the waste until system saturation. Then, the loading is led to the column until 10% of the maximum capacity was reached. DCB studies were also done in TOSOH Biosience laboratories.

3.3 – Flow microcalorimetry

The Microcalorimeter (Microscal Ltd, London, UK) can work under flow (FMC) or in a static mode (ITC).

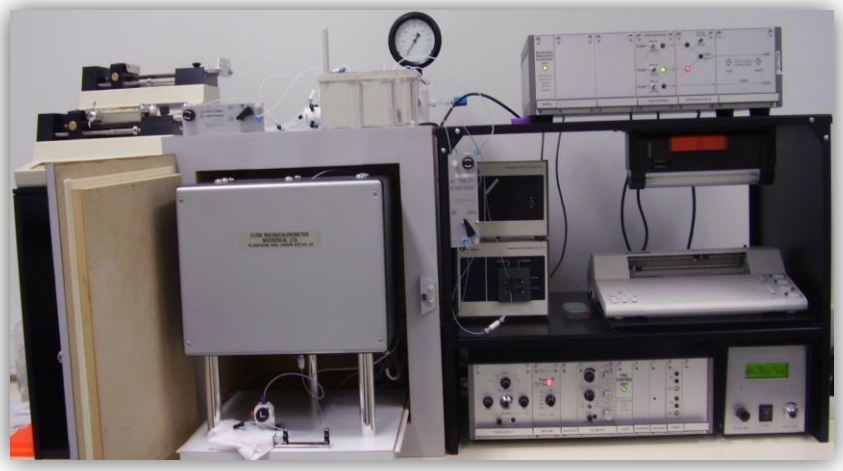

Figure 3.3.1 – Microcalorimeter (Microscal Ltd, London, UK) in a CICS-UBI laboratory.

FMC simulates a packed-bed chromatographic process allowing dynamic heat signal measurements. The column of 171µL is interfaced with two highly sensitive thermistors capable of detecting small temperature changes within the cell. The column was packed with a dried weight of the chromatographic supports to be studied, CMCand Toyopearl GigaCap-Q.

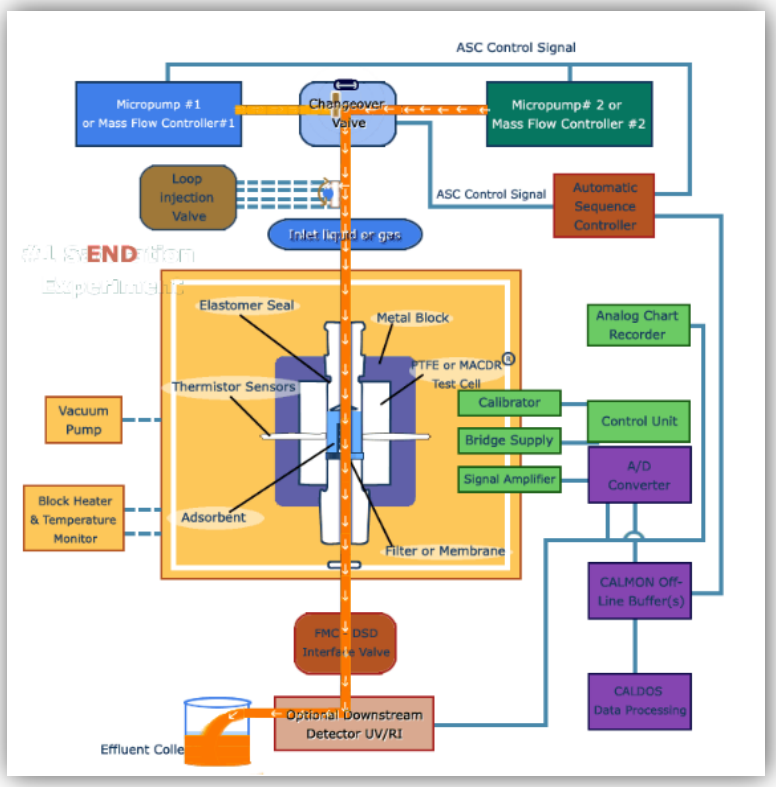

Figure 1 – Microcalorimeter schematic representation.

The system was then left to equilibrate at a constant flow rate of 1,5mL/h, controlled by precision syringe micropumps, with the different buffers: piperazine 20mM at pH 5 in the absence and in presence of 50mM NaCl for the CMC resin; Tris-HCl 20mM at pH 8 without salt for the anion exchanger. Lysozyme and BSA solutions were prepared in the respective buffers and injected in a configurable loop (30µL and 230µL) in a constant flow rate of 1,5mL. The effluent is collected and analysed with a UV spectrophotometer. A mass balance is calculated in order to know the adsorbed amount of protein. CALDOS 4 software is a program that acquires stores, calibrates, processes and presents the data of the interaction's enthalpy. The enthalpy is divided by the amount of protein adsorbed and plotted against protein surface concentration.

Chapter 4 - Discussion

4.1 - Static binding capacities for lysozyme and BSA adsorption onto ion-exchange resins at selected pH and different salt conditions

The study of adsorption isotherms is essential for the purpose of this work (understanding ion exhange adsorption mechanisms). So, isotherm measurements for lysozyme (Lys) adsorption onto a strong cation exchanger and bovine serum albumin (BSA) onto a weak and a strong anion exchanger were performed.

Lysozyme adsorption onto carboxymethyl cellulose, a strong cation exchanger, was carried at pH 5 in the absence of salt and in the presence of NaCl 50mM. The collected data is presented in Figure 4.1.1 and 4.1.2. Figure 4.1.2 represents a "zoom in" of the low protein equilibrium concentration zone. It can be seen that in this region the shape of the curve is similar to the Langmuir isotherm profile [25].

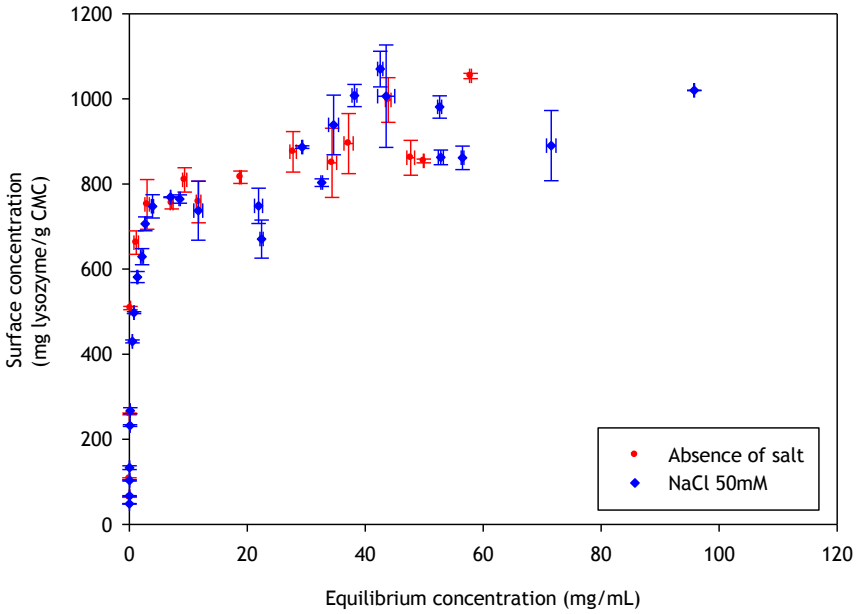

Figure 4.1.1 - Adsorption isotherms for lysozyme on carboxymethyl cellulose at pH 5 in piperazine buffer; Red circles: Absence of salt; Blue diamonds: 50mM NaCl.

As expected due to the screening effect of NaCl, lysozyme surface concentration is greater in the absence of salt for low protein equilibrium concentrations. Also, lysozyme distribution

coeficient in the isotherm linear region, under these conditions, is higher when compared to the presence of salt [12].

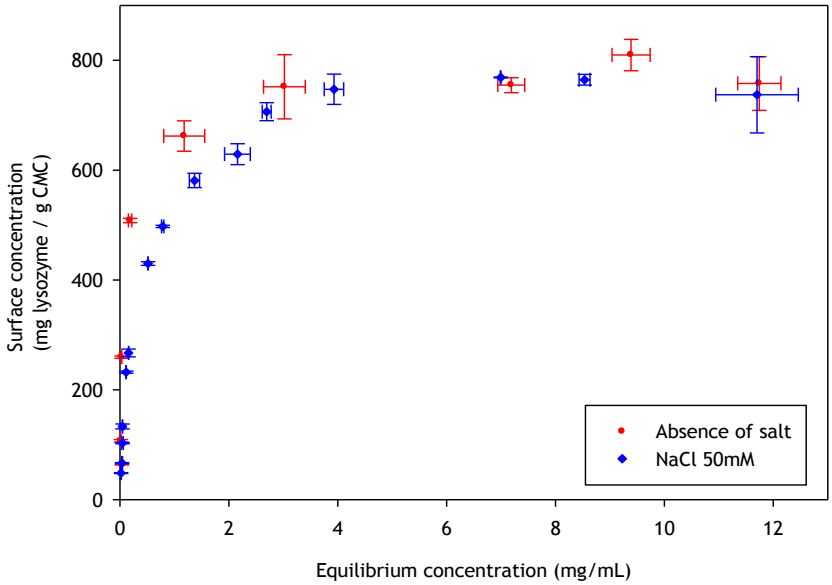

Figure 4.1.2 - "Zoom in" of the initial concentrations of the isotherm for lysozyme on carboxymethyl cellulose at pH 5 in piperazine buffer; Red circles: Absence of salt; Blue diamonds: 50mM NaCl.

Analysing the whole curve profile (Figure 4.1.1), it can be seen that for both conditions (presence and absence of salt) with increasing protein equilibrium liquid concentrations an increase from zero capacity to a plateau region is observed. This plateau is followed by a region of increasing capacity, indicating the formation of multi-layers of lysozyme on the surface or a reorientation of the adsorbed protein to accommodate more molecules. The alteration of conformation of adsorbed lysozyme is here excluded once this protein is considered to have a high degree of structural stability [61]. It has been reported by some autors that lysozyme suffers dimerisation in a pH range 5 to 9 [62]. However, having its isoelectric point at around 11 [63], at pH 5 the protein is fully charged. This higher density of charges causes some repulsion between lysozyme molecules, making dimer formation more difficult [64]. Therefore, at these working conditions the monomer-dimer equilibrium is likely to be displaced to the monomer state.

Another interesting feature of the adsorption isotherms is observed in the region of the increasing capacity following the plateau (Figure 4.1.1). In this region lysozyme surface concentration seems to be greater in the presence of 50mM of NaCl. This behaviour may also be explained by salt screening effect under overloaded conditions. Here, two mechanisms might promote lysozyme adsorption: multi-layer formation or protein reorientation. Both mechanisms are favoured when repulsion between charged proteins is reduced, which is achieved in the presence of low salt concentrations.

BSA adsorption isotherms measurements were performed at different working conditions according to the resin used. For Toyopearl DEAE-650M resin, a weak anion exchanger, pH 8 was used. For the strong exchanger, Toyopearl GigaCap Q-650M, the experiments were carried at pH 9. As already mentioned, in order to evaluate the salt effect, for both resins three different salt conditions were tested, 0, 50mM and 100mM NaCl. Figures 4.1.3 and 4.1.4 show the isotherm results for BSA adsorption onto GigaCap Q-650M.

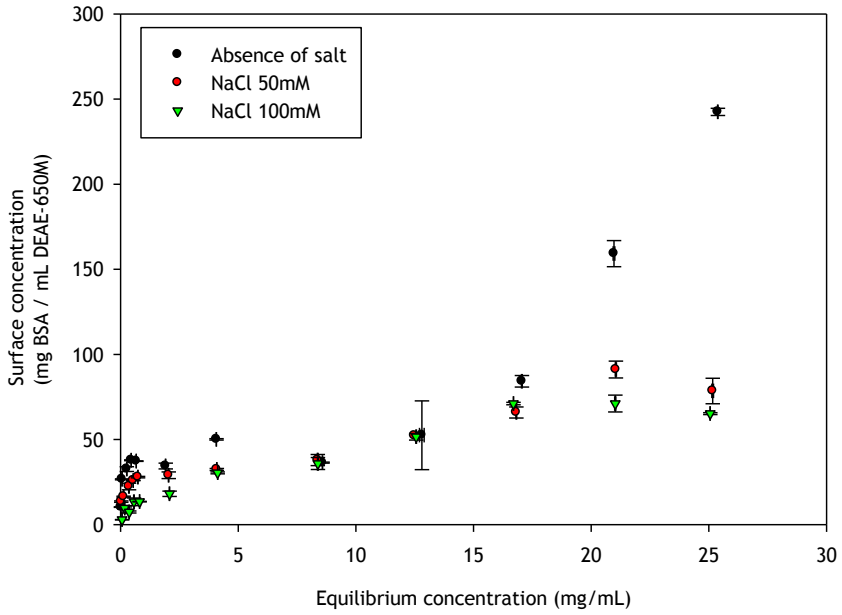

Figure 4.1.3 - Adsorption isotherms for BSA onto Toyopearl DEAE-650M. Buffer: Tris 20mM, pH 8; Black: Absence of salt; Red: 50mM; Green: 100mM NaCl.

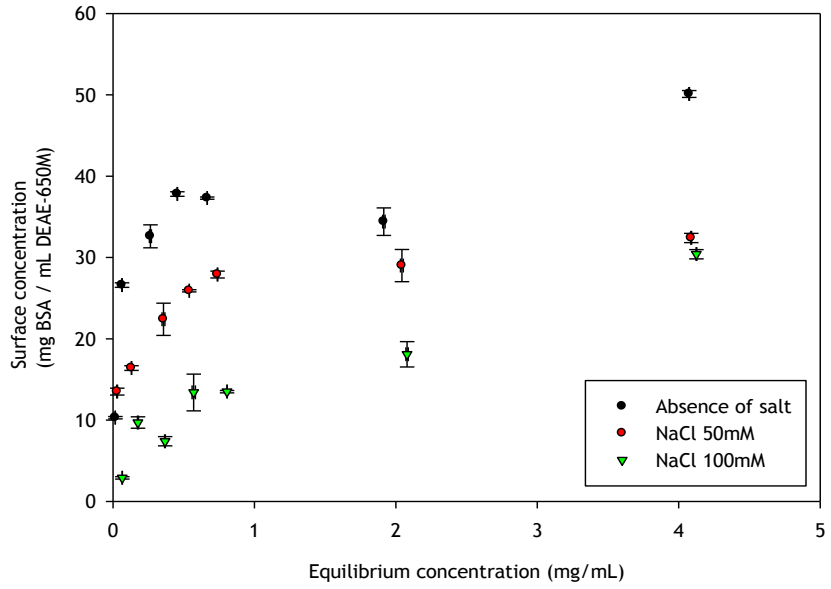

Figure 4.1.4 - "Zoom in" of the initial concentrations of the adsorption isotherms for BSA onto Toyopearl DEAE-650M. Buffer: Tris 20mM, pH 8; Black: Absence of salt; Red: 50mM; Green: 100mM NaCl.

As expected for an electrostatic adsorption mechanism, as the salt concentration increases the amount that is adsorbed decreases. At every salt concentration, with increasing protein equilibrium concentrations an increase from zero capacity to a plateau region is observed. Static binding capacities between 25mg/mL (for 100 mM NaCl) and 40mg/mL (in absence of salt) were reached in this zone. In the absence of salt, this plateau is followed by a region of rapidly increasing capacity. Contrariwise, in the presence of salt a second plateau is reached, showing higher capacity at 50mM NaCl. By analysis of these data along with enthalpic data, an explanation for this behaviour may be advanced. Multi-layer formation, protein reorientation or alteration of conformation as BSA is considered a "soft" molecule [65,66], are plausible hypothesis.

The GigaCap Q-650M resin showed a more rectangular Langmuir isotherm shape than DEAE-650M resin for the lowest protein equilibrium concentrations (Figures 4.1.5 and 4.1.6), which is not strange as the later support is considered a weak anion exchanger. In addition, just like the DEAE-650M resin isotherm profile, GigaCap Q-650M isotherm seems to reach a first plateau but regardless the salt concentration used a second plateau is never achieved. As said before, several processes maybe present as it will be explained later by FMC analysis. Also, it should be kept in mind that GigaCap Q-650M is a polymer modified support. Therefore it allows a better access to the ligand binding sites, resulting in higher adsorption capacities than the DEAE-650M resin [10,11].

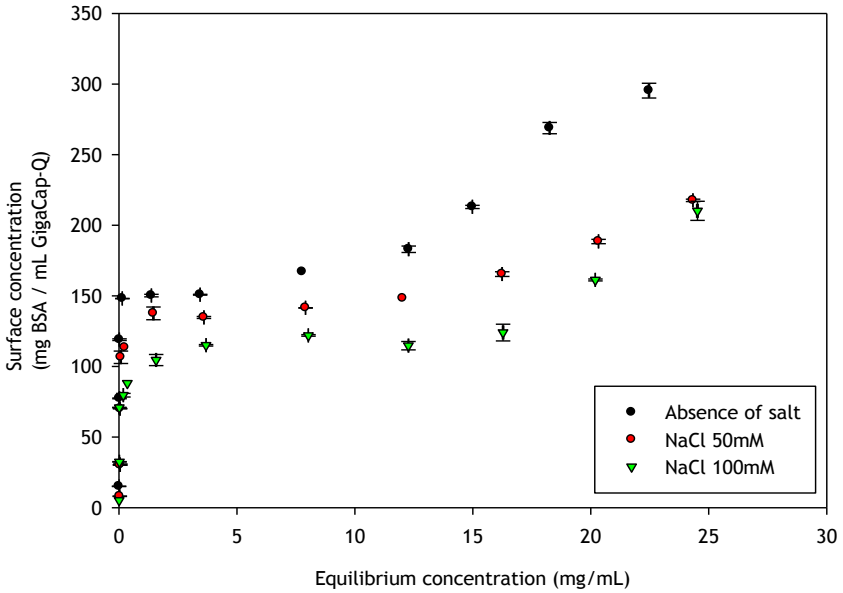

Figure 4.1.5 - Adsorption isotherms for BSA onto Toyopearl GigaCap-Q. Buffer: Tris 20mM, pH 9; Black: Absence of salt; Red: 50mM; Green: 100mM NaCl.

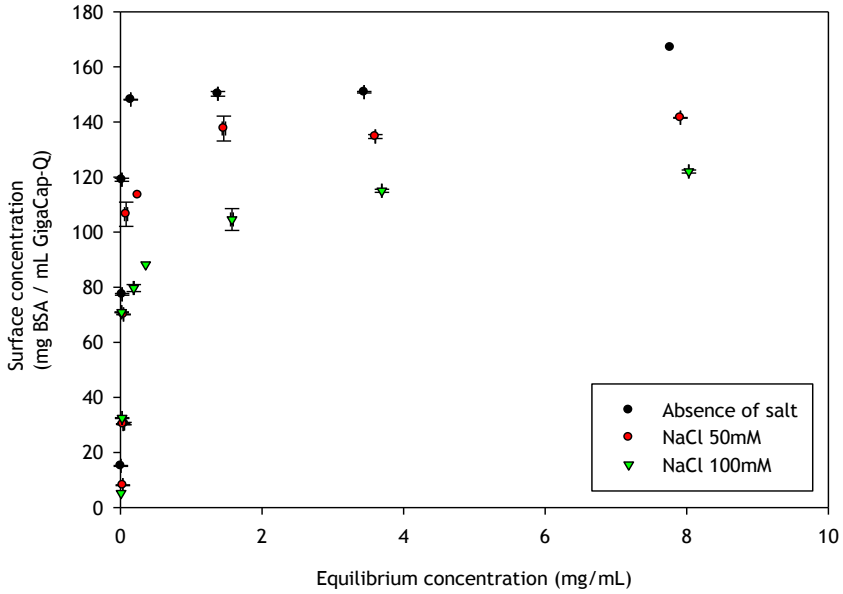

Figure 4.1.6 - "Zoom in" of the initial concentrations of the adsorption isotherms for BSA onto Toyopearl GigaCap-Q. Buffer: Tris 20mM, pH 9; Black: Absence of salt; Red: 50mM; Green: 100mM NaCl.

4.2 - Dynamic binding capacities for BSA adsorption onto anion exchange resins at different pH and salt conditions

The dynamic binding capacities of the two resins (Toyopearl DEAE-650M and Toyopearl GigaCap-Q) were determined by frontal analysis of pure BSA using different working conditions and a constant flow rate of 150cm/h. Figure 4.2.1 show the results for the DEAE-650M resin as function of the different salt, pH and protein conditions used.

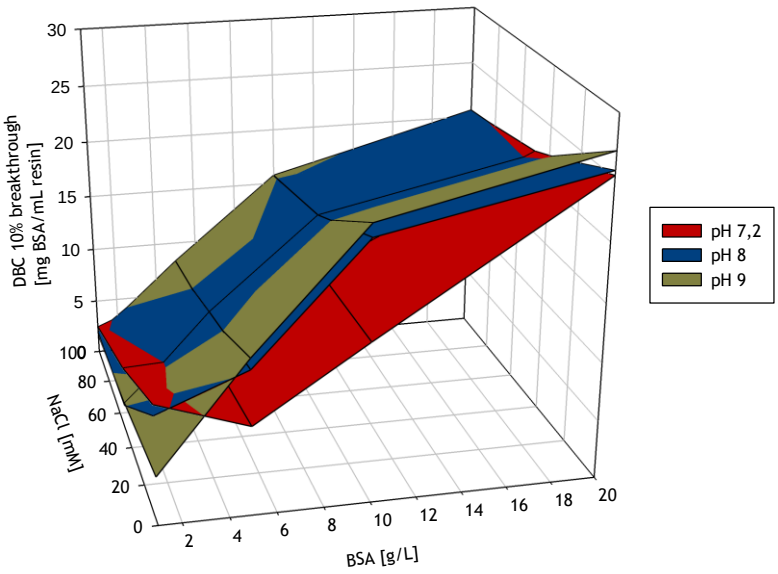

Figure 4.2.1 - Dynamic binding capacities results for Toyopearl DEAE-650M for BSA. Buffer: Tris 20mM (0, 50mM and 100mM NaCl); pH 7,2, 8 and 9; BSA concentration 1-20g/L; Flow rate 150cm/h.

Overall, the dynamic binding capacity values for both resins were low. Both at low and high protein concentrations, the DEAE-650M resin showed a dependency on salt concentration, consistent with an ion exchange adsorption mechanism. The best results were obtained at pH 8 and 9, under which BSA is more negatively charged. DBC are similar at these two pH, even though BSA's negative charge is greater at pH 9. The binding capacity of DEAE-650M for BSA stated in the product specifications is 25mg/mL for a protein loading of 1mg/mL and flow rate 212cm/h. This value was only obtained when working with high protein concentrations.

Figure 4.2.2 shows the collected data for the DBC experiments in the GigaCap-Q adsorbent.

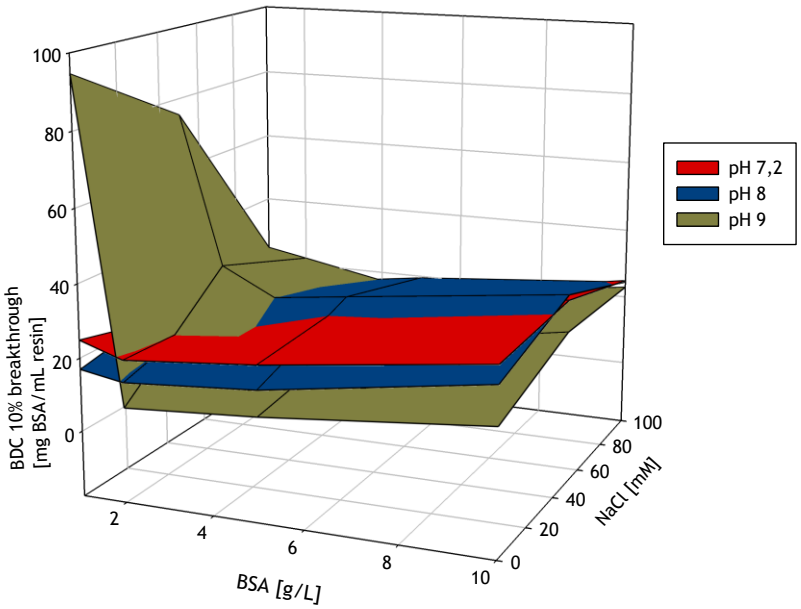

Figure 4.2.2 - Dynamic binding capacities results for Toyopearl GigaCap-Q for BSA. Buffer: Tris 20mM (0, 50mM and 100mM NaCl); pH 7,2, 8 and 9; BSA concentration 1-20g/L. Flow rate 150cm/h.

Just like the reference data (173mg BSA/mL resin for a protein loading of 1mg/mL at a flow rate of 212cm/h), the experimental binding capacities results for the grafted resin – GigaCap-Q – were, as expected, generally higher than for the non-grafted. GigaCap-Q is a polymer modified resin, thus improving the accessible location of the ligand groups, resulting in an increased binding capacity. Unlike the non-grafted DEAE resin, GigaCap-Q appears to have a linear increasing binding capacity according to protein concentration. However, at pH 9, for 1 mg/mL loading and in the absence of NaCl the resulted binding capacity was 95 mg/mL, 4-5 times higher than the capacity obtained for higher protein concentrations. Also, the presence of mild ionic strength seems to have a different effect on the adsorption capacity of this resin, since that the best results were often obtained in the presence of 50mM of NaCl.

These strange outcomes, confirmed by the generally low binding capacity results obtained for both resins may probably result from the lack of column regeneration. After washing with sodium hydroxide 200mM, column regeneration with HCl should have been done.

4.3 - Microcalorimetry to investigate the surface phenomena

As already stated, overall adsorption in ion exchange chromatography is expected to be an exothermic process [9]. However, the adsorption mechanism of IEC is more complex, since there are several kinds of interactions that can occur, resulting in endothermic heats.

On one hand, ion exchange chromatography is based on electrostatic interactions between the stationary phase and the oppositely charged target molecule. This attraction leads to energy releasing, making IEC adsorption an exothermic interaction. On the other hand, endothermic phenomena can also occur. Among the sources for endothermic heats there are repulsive interactions between adsorbed molecules, repulsive interactions between protein surface hydrophobic groups and adsorbent surface hydrophilic moieties, repulsive interactions between like charge groups on the protein surface and on the adsorbent surface, water release from adsorbent's and protein's surface, protein conformational changes and protein reorientation on the surface [2].

This work was performed in order to understand Lys and BSA adsorption onto different ion exchangers and to check the effect of salt in a specific pH and for a wide range of protein concentrations; from the linear zone to oversaturation.

Starting with lysozyme adsorption onto CMC, as already described in the Experimental section, because of the limitations with lysozyme solubility, two different loops (30µL and 230µL) were used in order to reach higher protein surface concentrations. Despite the difference in the volume of the loop the flow rate was always kept constant at 1,5mL/h, resulting in differences in the residence time of the molecules in the system. Thus, the results have to be discussed according to loop used as it will be explained later.

In the experiments performed at pH 5 in piperazine buffer using the 30µL loop, lysozyme initial concentration varied in the range 20-320mg/mL in the no salted buffer and 30-350mg/mL in the presence of 50mM of NaCl. Figures 4.3.1 and 4.3.2 show the heat signal profile of the injections at the mentioned conditions in the absence of NaCl, resulting in surface concentrations from ~30 to 145mg lysozyme/g CMC. Figures 4.3.12 and 4.3.13 represent the heat signal profile of some of the injections in 50mM NaCl, which resulted in surface concentrations from ~50 to 155mg lysozyme/g CMC.

As referred, Figures 4.3.1, 4.3.2, 4.3.12 and 4.3.13 show two different perspectives of the thermogram profile resulting from the microcalorimetric experiments run with a 30µL loop both in absence and presence of salt. As it can be observed, there are distinct events: firstly, a small exothermic interaction seems to take place; then, there are overlapping endothermic peaks; finally, an exothermic heat can be seen. As these processes may be occurring simultaneously or sequentially, MATLAB de-convolution is needed. After each thermogram

profile for both working conditions, the data analysed with MATLAB software is shown. Figures 4.3.3 to 4.3.11 for the no salted injections and 4.3.14 to 4.3.19 for the presence of 50mM of sodium chloride show the de-convolution of the heat signals recorded by CALDOS for the experiments with the 30µL loop. This tool allows taking in account the energetic events that were apparently disguised by CALDOS software.

It is useful to analyse the trends within the framework of the mechanism defined by Lin and co-workers [54,63,67], who suggested that ion exchange adsorption can be divided into five sequential sub-processes:

i) water molecules and ion release from the protein surface;

ii) water molecules and ion release from the adsorbent surface;

iii) electrostatic and/or hydrophobic interactions between protein and the ion exchanger;

iv) structural conformation rearrangement and reorientation of the adsorbed protein;

v) rearrangement of the excluded water molecules and ions in a the solution.

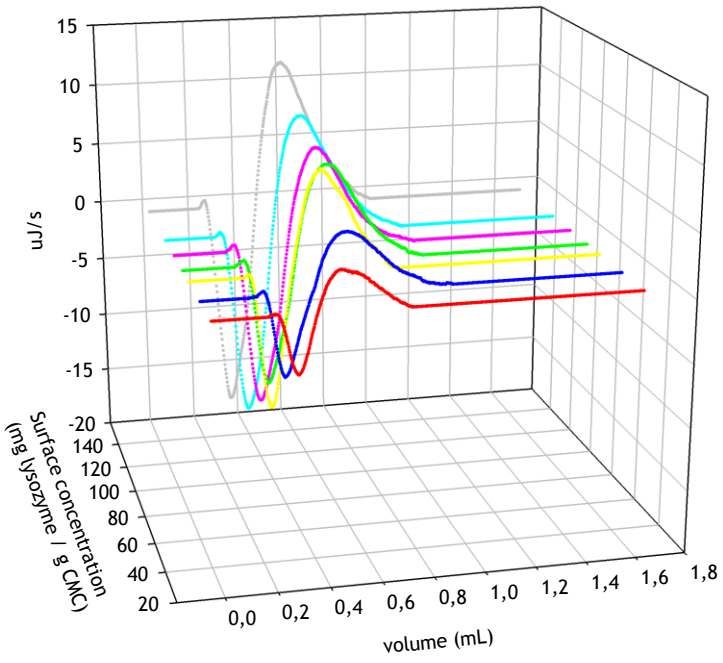

Figure 4.3.1 - Thermograms of lysozyme adsorption on carboxy-methyl cellulose at pH 5 in piperazine buffer 20mM in the absence of salt using a loop with 30µL; Red - 31,4mg lysozyme/g CMC; Blue - 49,1mg/g; Yellow - 67,9mg/g; Green - 78,9mg/g; Pink - 94,4mg/g; Cyan - 111,0mg/g; Grey - 144,5mg/g.

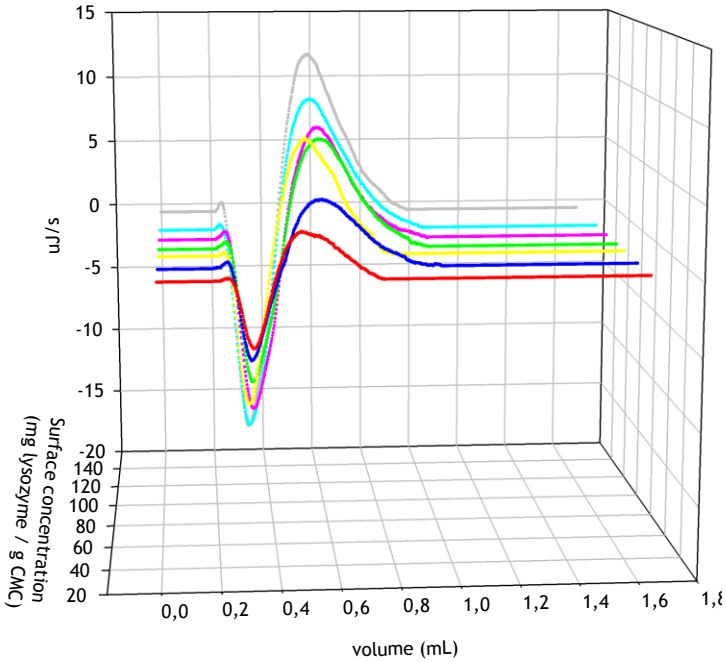

Figure 4.3.2 - Different perspective of the thermograms of lysozyme adsorption on carboxy-methyl cellulose at pH 5 in piperazine buffer 20mM in the absence of salt using a loop with 30µL.

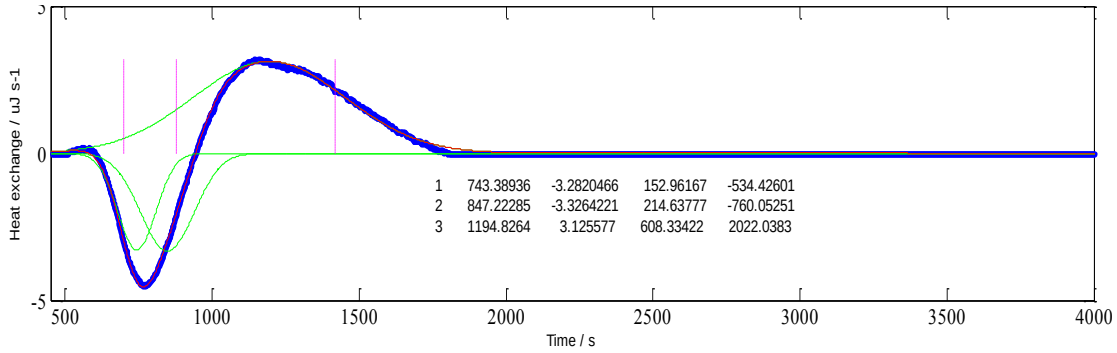

Figure 4.3.3 - MATLAB de-convolution of the thermograms of lysozyme adsorption on carboxy-methyl cellulose at pH 5 in piperazine buffer 20mM using a loop of 30µL. Surface concentration: 31,4mg/g.

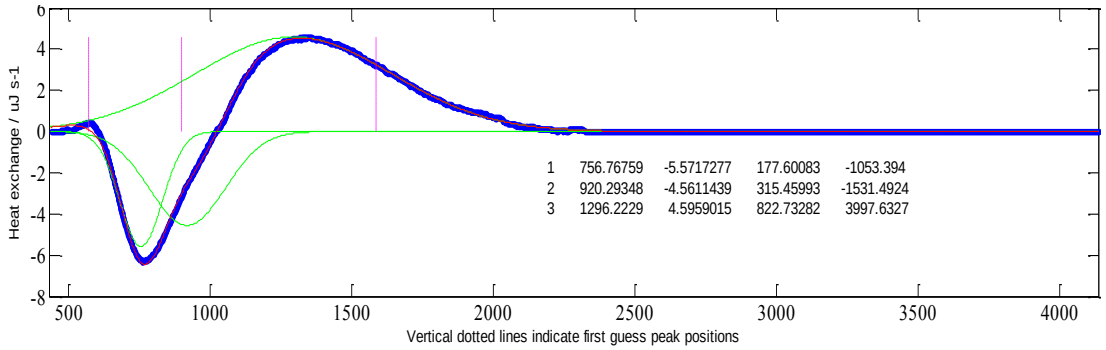

Figure 4.3.4 – MATLAB de-convolution of the thermograms of lysozyme adsorption on carboxy-methyl cellulose at pH 5 in piperazine buffer 20mM using a loop of 30µL. Surface concentration: 49,1mg/g

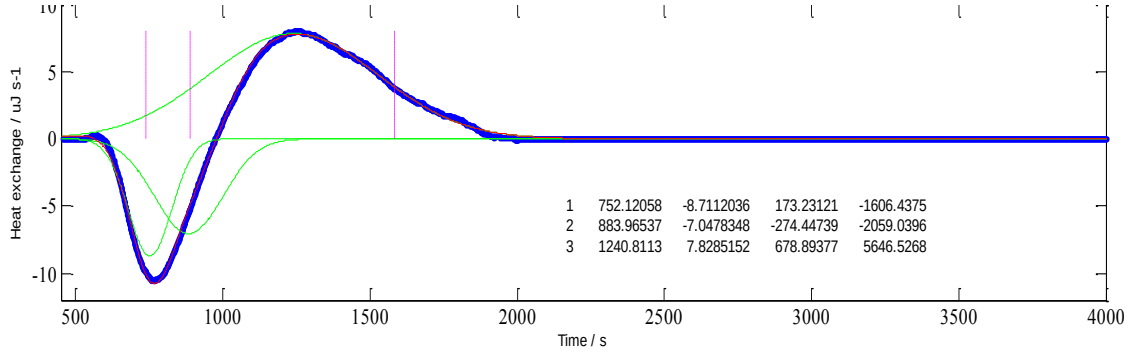

Figure 4.3.5 – MATLAB de-convolution of the thermograms of lysozyme adsorption on carboxy-methyl cellulose at pH 5 in piperazine buffer 20mM using a loop of 30µL. Surface concentration: 67,9mg/g

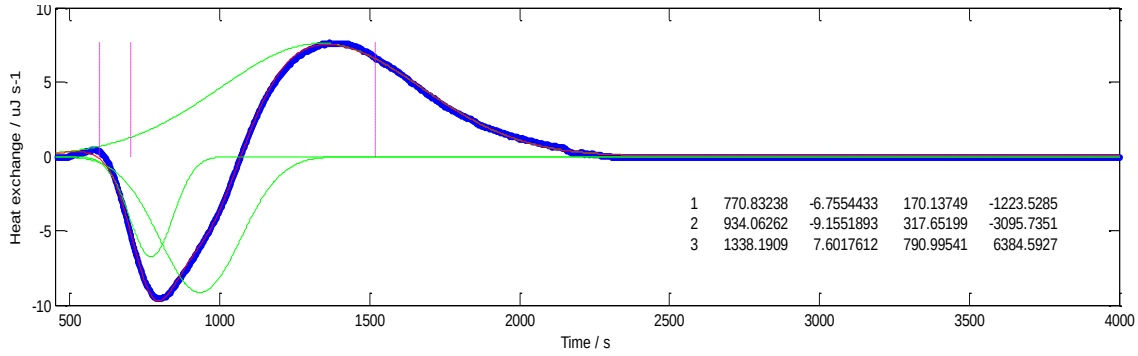

Figure 4.3.6 – MATLAB de-convolution of the thermograms of lysozyme adsorption on carboxy-methyl cellulose at pH 5 in piperazine buffer 20mM using a loop of 30µL. Surface concentration: 78,9mg/g

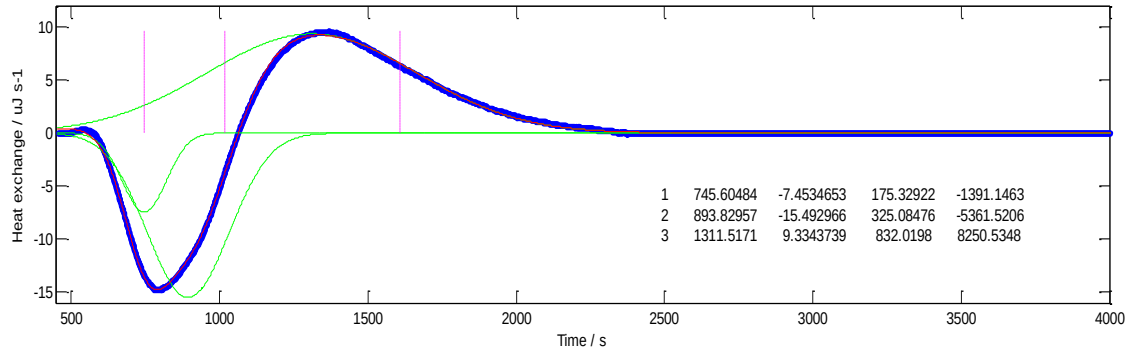

Figure 4.3.7 - MATLAB de-convolution of the thermograms of lysozyme adsorption on carboxy-methyl cellulose at pH 5 in piperazine buffer 20mM using a loop of 30µL. Surface concentration: 111,0mg/g

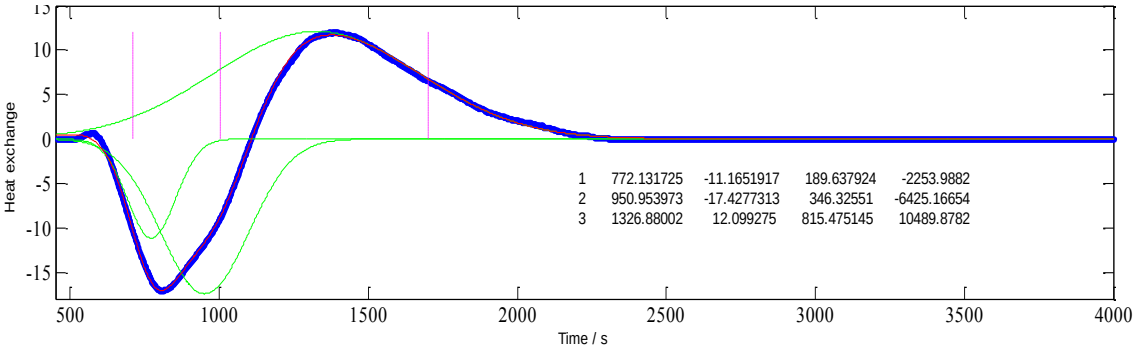

Figure 4.3.8 - MATLAB de-convolution of the thermograms of lysozyme adsorption on carboxy-methyl cellulose at pH 5 in piperazine buffer 20mM using a loop of 30µL. Surface concentration: 144,5mg/g

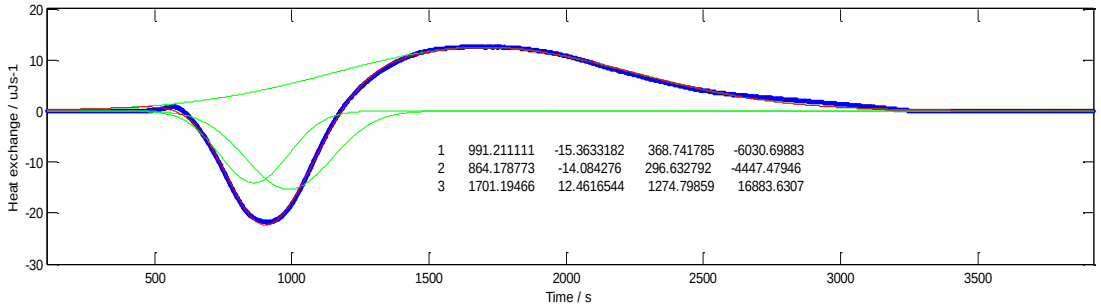

Figure 4.3.9 - MATLAB de-convolution of the thermograms of lysozyme adsorption on carboxy-methyl cellulose at pH 5 in piperazine buffer 20mM using a loop of 30µL. Surface concentration: 152,7mg/g

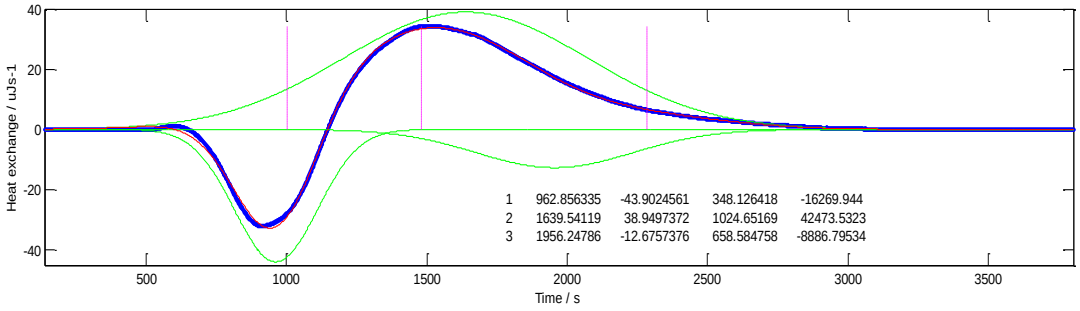

Figure 4.3.10 - MATLAB de-convolution of the thermograms of lysozyme adsorption on carboxy-methyl cellulose at pH 5 in piperazine buffer 20mM using a loop of 30µL. Surface concentration: 217,4mg/g

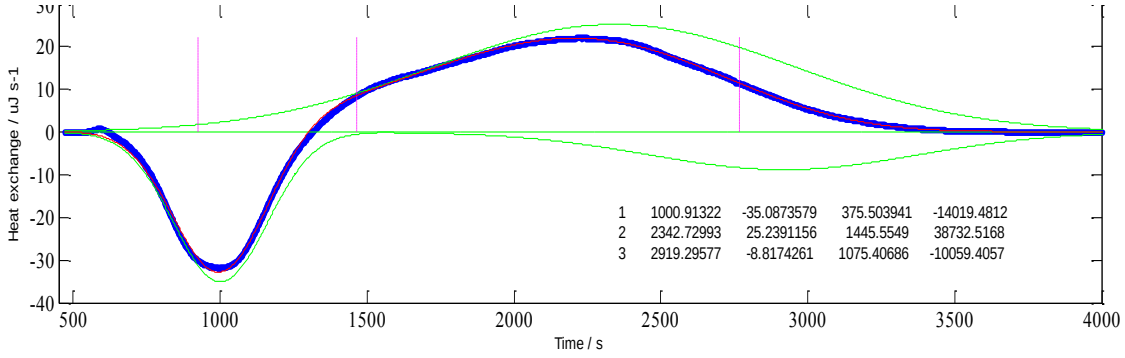

Figure 4.3.11 - MATLAB de-convolution of the thermograms of lysozyme adsorption on carboxy-methyl cellulose at pH 5 in piperazine buffer 20mM using a loop of 30µL. Surface concentration: 313,7mg/g

From the thermograms, it can be seen that few moments after the injection, a first exothermic interaction seems to take place. This point corresponds to the exact moment at which the front of the protein solution reaches the resin in the cell. Since the resin surface is negatively charged and the protein is positively charged at pH 5, adsorption of the protein to the ion exchanger occurs. The energetic values at this point increase with protein surface concentration. In the presence of salt, this moment happens on the twelfth minute (0,3mL). Without salt, though, shorter tubing was used, an earlier first interaction was observed (minute 9; 0,23mL).

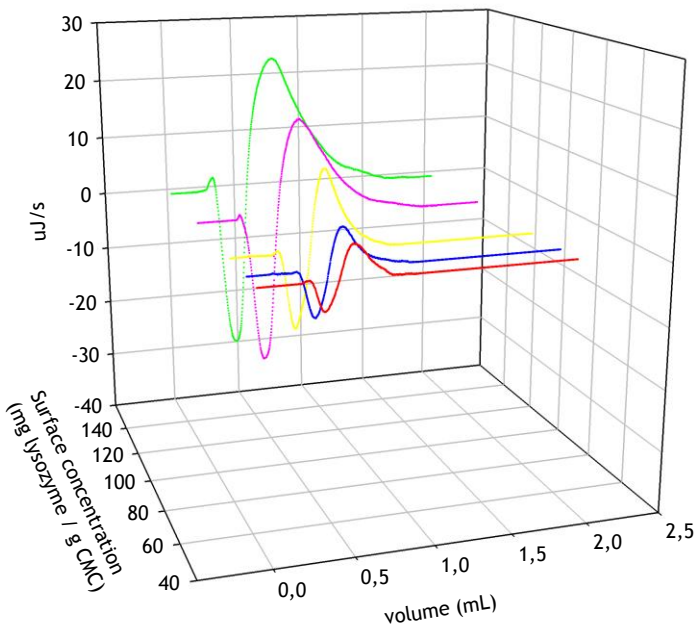

Figure 4.3.12 - Thermograms of lysozyme adsorption on carboxy-methyl cellulose at pH 5 with 50mM NaCl in piperazine buffer 20mM using a loop of 30µL; Red – 50,7 mg lysozyme/g CMC; Blue – 60,6mg/g; Yellow – 77,8mg/g; Pink – 116,1mg/g; Green – 153,6mg/g.

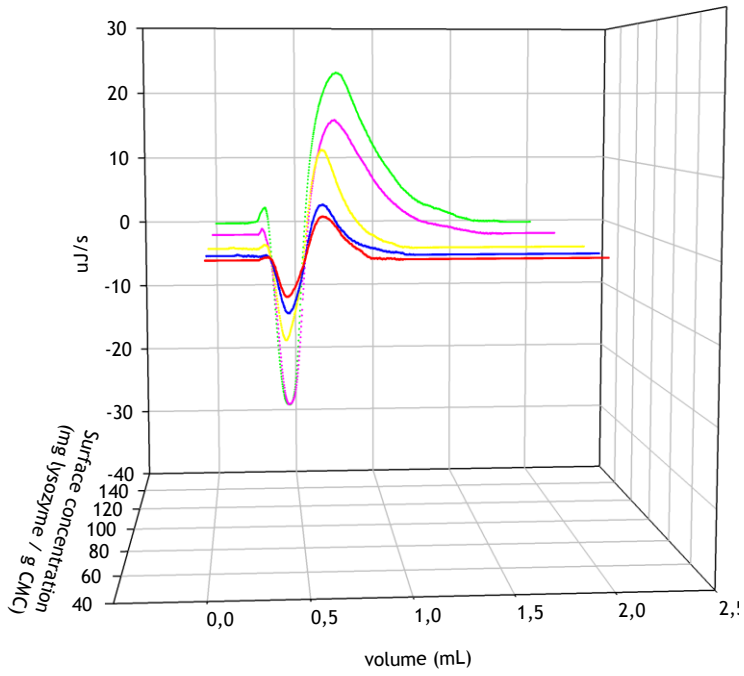

Figure 4.3.13 - Different perspective of the thermograms of lysozyme adsorption on carboxy-methyl cellulose at pH 5 with 50mM NaCl in piperazine buffer 20mM using a loop of 30µL.

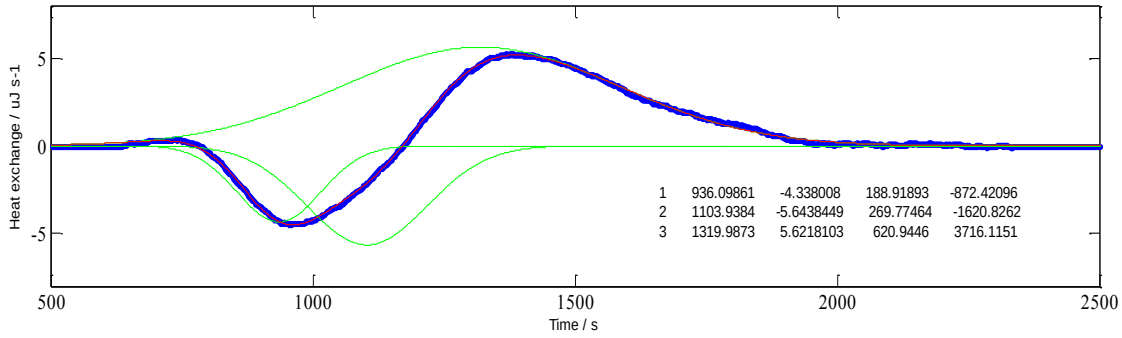

Figure 4.3.14 - MATLAB de-convolution of the thermograms of lysozyme adsorption on carboxy-methyl cellulose at pH 5 with 50mM NaCl in piperazine buffer 30mM using a loop of 30µL. Surface concentration: 50,7mg/g

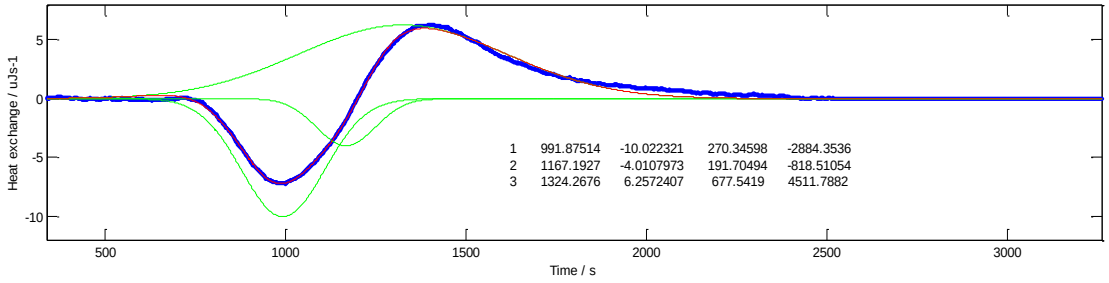

Figure 4.3.15 - MATLAB de-convolution of the thermograms of lysozyme adsorption on carboxy-methyl cellulose at pH 5 with 50mM NaCl in piperazine buffer 20mM using a loop of 30µL. Surface concentration: 60,6mg/g

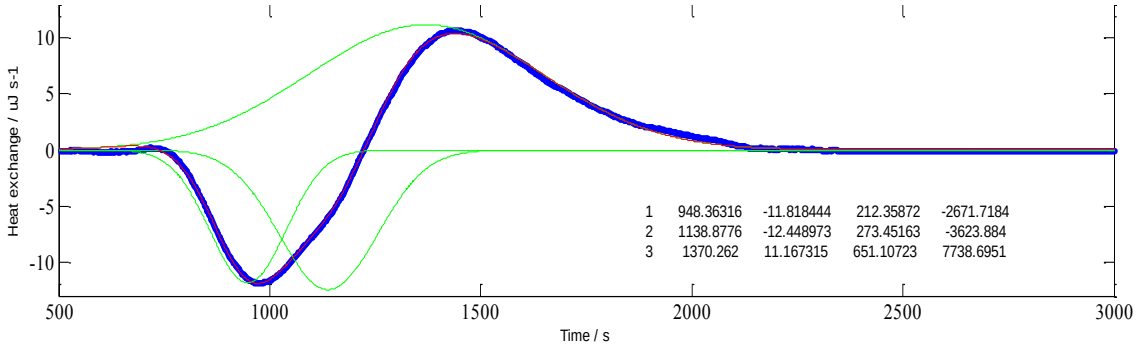

Figure 4.3.16 - MATLAB de-convolution of the thermograms of lysozyme adsorption on carboxy-methyl cellulose at pH 5 with 50mM NaCl in piperazine buffer 20mM using a loop of 30µL. Surface concentration: 85,4mg/g

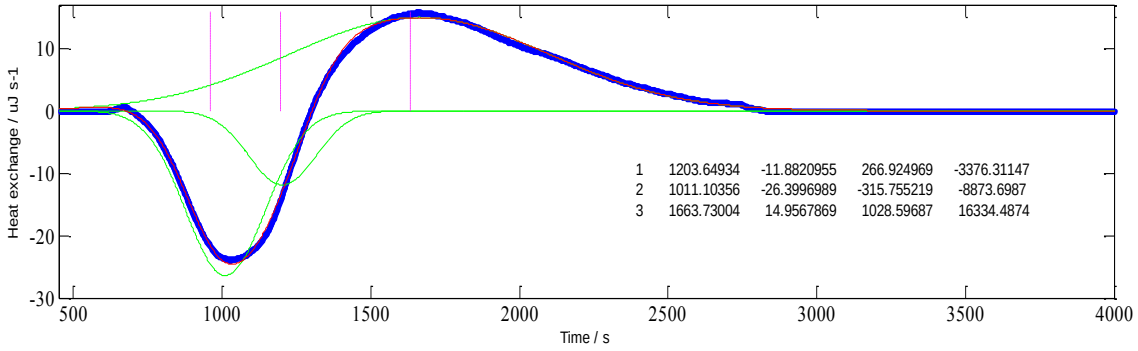

Figure 4.3.16 - MATLAB de-convolution of the thermograms of lysozyme adsorption on carboxy-methyl cellulose at pH 5 with 50mM NaCl in piperazine buffer 20mM using a loop of 30µL. Surface concentration: 114,9mg/g

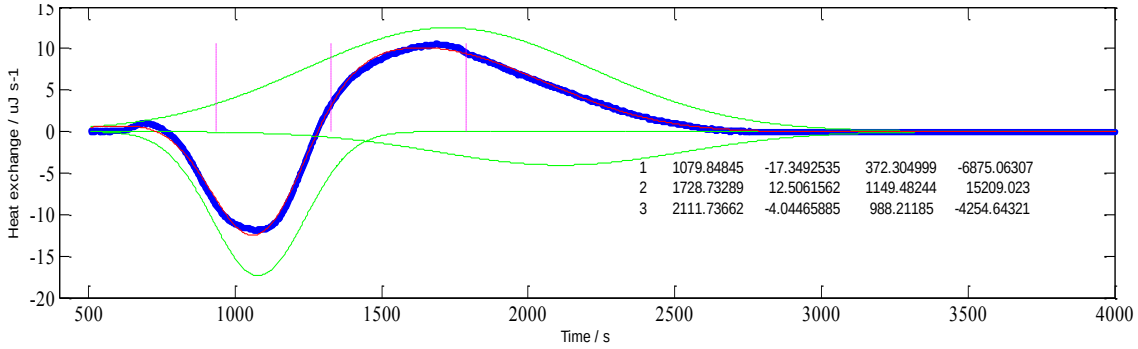

Figure 4.3.17 - MATLAB de-convolution of the thermograms of lysozyme adsorption on carboxy-methyl cellulose at pH 5 with 50mM NaCl in piperazine buffer 20mM using a loop of 30µL. Surface concentration: 129,2mg/g

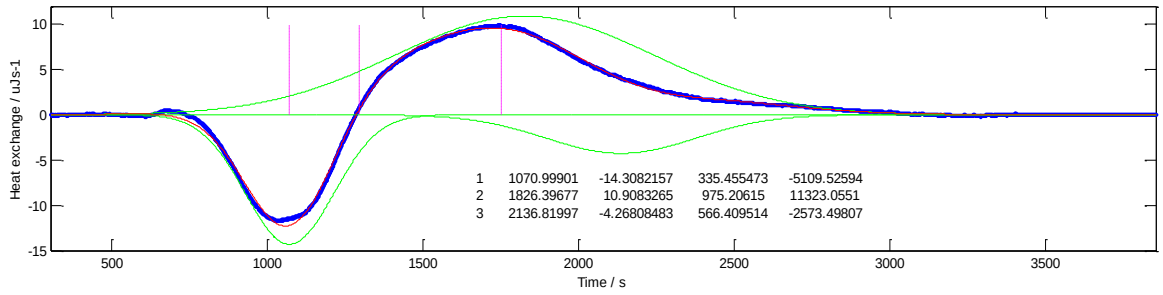

Figure 4.3.18 - MATLAB de-convolution of the thermograms of lysozyme adsorption on carboxy-methyl cellulose at pH 5 with 50mM NaCl in piperazine buffer 20mM using a loop of 30µL. Surface concentration: 154,5mg/g

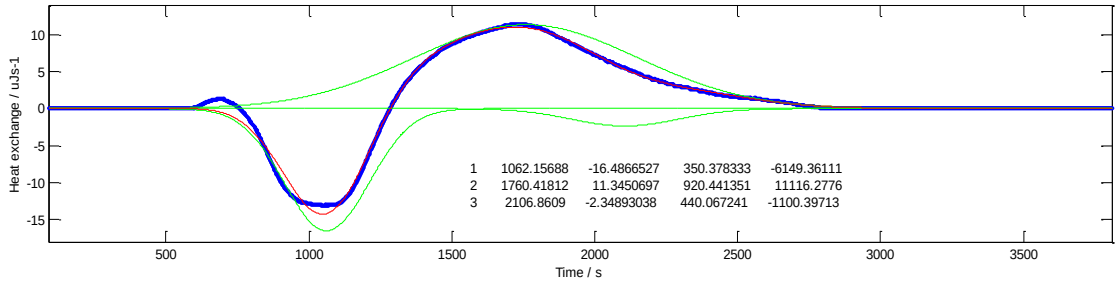

Figure 4.3.19 - MATLAB de-convolution of the thermograms of lysozyme adsorption on carboxy-methyl cellulose at pH 5 with 50mM NaCl in piperazine buffer 20mM using a loop of 30µL. Surface concentration: 183,9mg/g

As shown with MATLAB, two overlapping endothermic peaks are present. A possible source for the first endothermic signal is the release of counterions and, in a less extent, water molecules from lysozyme and adsorbent surface, causing an increase of energy in the chromatographic system. This allows lysozyme adsorption.

The explanation for the second peak may be related with reorientation of surface molecules and/or repulsion between adsorbed biomolecules. For both, in absence and in presence of salt, as protein surface concentration increases, the maximum of the second endothermic peak appears later in time. Lysozyme has a preferred binding position for cation exchangers [68–70] so it is expected the reorientation of surface molecules in favour of that orientation. With increasing protein surface coverage, is predictable a Lys rotation from a space-consuming to a space saving orientation [68,69]. Also interesting to observe is the fact that at approximately the same surface coverage, in presence (Figure 4.3.18) and in absence of salt (Figure 4.3.9), the second endothermic peak maximum appears sooner when salt is not present, behaviour consistent with a higher repulsion between the adsorbed biomolecules that are fully charged under this condition and promotes re-orientation sooner.

In the experiments run with the 30µL loop (Figure 4.3.20), by comparing the enthalpy of the first endothermic heat as function of surface concentration in absence and presence of salt, it can be seen that at low protein concentrations, there are no significant differences. Since the source for the first heat is assumed to be ion and water molecules release from protein and adsorbent surface, the balance of these events seems similar for both conditions. It is well known that the increase of ionic strength reduces double layer thickness, being expected a reduction in the positive enthalpy, however if more water molecules are released this effect may be masked. [55,57].

By looking at the enthalpy of the second endothermic heat as function of surface concentration (Figure 4.3.21), there is a clear sharp maximum probably associated with lysozyme reorientation at the surface of the adsorbent in the presence of salt. It should be kept in mind that this maximum occurs at the zone of the isotherm at which it starts to level,

indicating saturation of the resin. Once we are in presence of salt, it is expected more protein reorientation than in its absence, because of the salt shielding already explained.

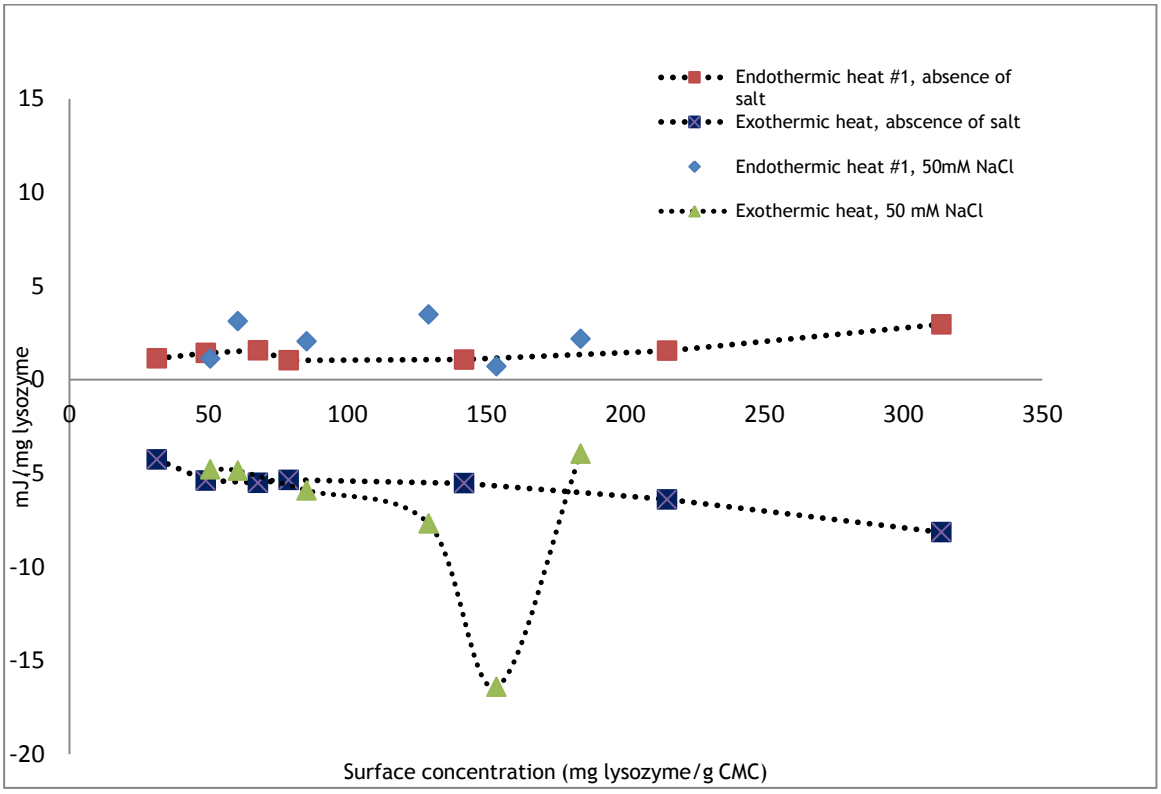

Figure 4.3.20 - Microcalorimetric results of the first endothermic peak and the exotherm for the experiments performed with the 30µL loop, with and without salt.

Back to the explanation of peak profile (Figures 4.3.1, 4.3.2, 4.3.12 and 4.3.13) a high exothermic process seems to occur. The peak is broad and gets some tailing as surface concentration increases. After de-convolution, it is found that this exothermic process is fully overlapped with the endothermic signals. This event corresponds to adsorption itself and, as it can be seen in Figure 4.3.20 as we are getting away from the linear zone of the isotherm the exothermic interaction becomes more energetic for both salt conditions, however with different trends. While in the absence of salt the exothermic heat increases linearly, in presence of 50mM NaCl there is a well-defined minimum and then a sudden increase. The sharp minimum can be justified by the increased reorientation process near the first plateau in the isotherm (Figure 4.1.1). The process of reorientation is enthalpically driven due to attractive interactions between adsorbed molecules at high surface coverage. The exothermic heat of adsorption would increase when the degree of reorientation increases, near the plateau, and would decrease as the monolayer capacity is reached.

By looking to the net heat of both experiments (4.3.22 to 4.3.24), we can see that despite the ionic strength, for low protein surface concentrations, the reaction is equally stronger. This is

expected since the resin, under these conditions is not saturated and protein is free to attach. Nonetheless, when a certain protein concentration is reached (~150mg/g), there is a maximum of energy release in the presence of salt. As discussed before this can be explained by reorientation, as this process is an enthalpicay driven one. Anyway under both conditions, presence and absence of salt, global process is enthalpically driven as expected for a strong cation exchanger like CMC.

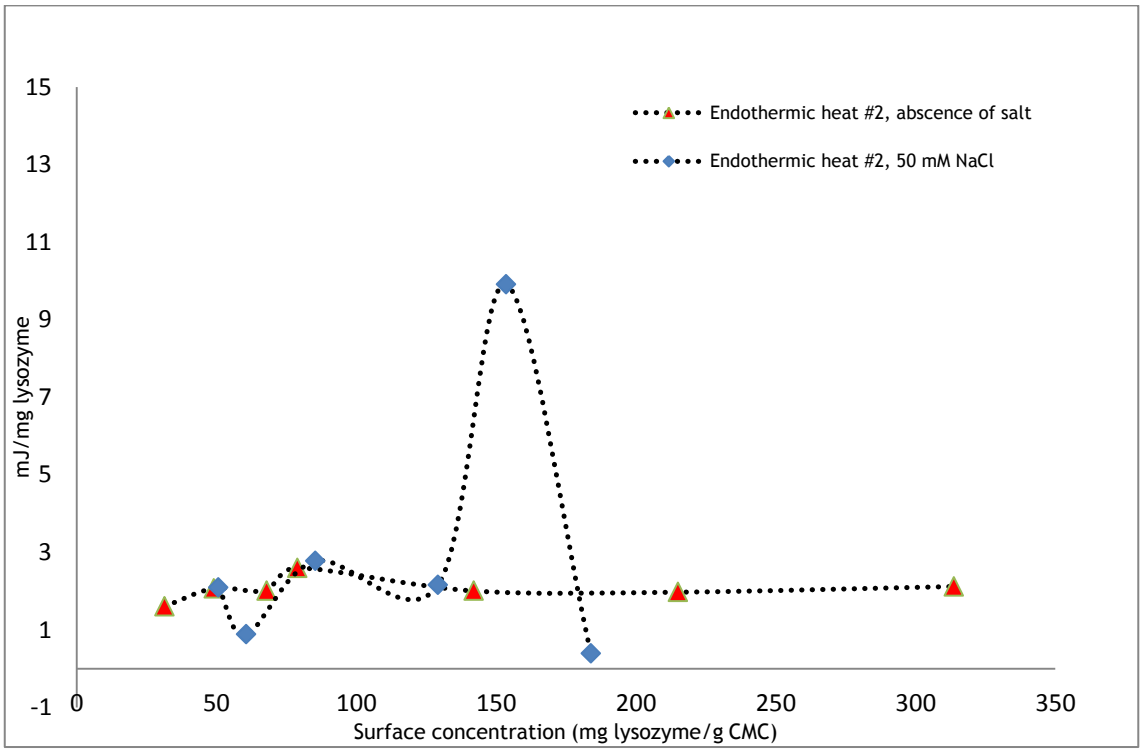

Figure 4.3.21 – Microcalorimetric results of the second endothermic peak for the experiments performed with the 30µL loop, with and without salt.

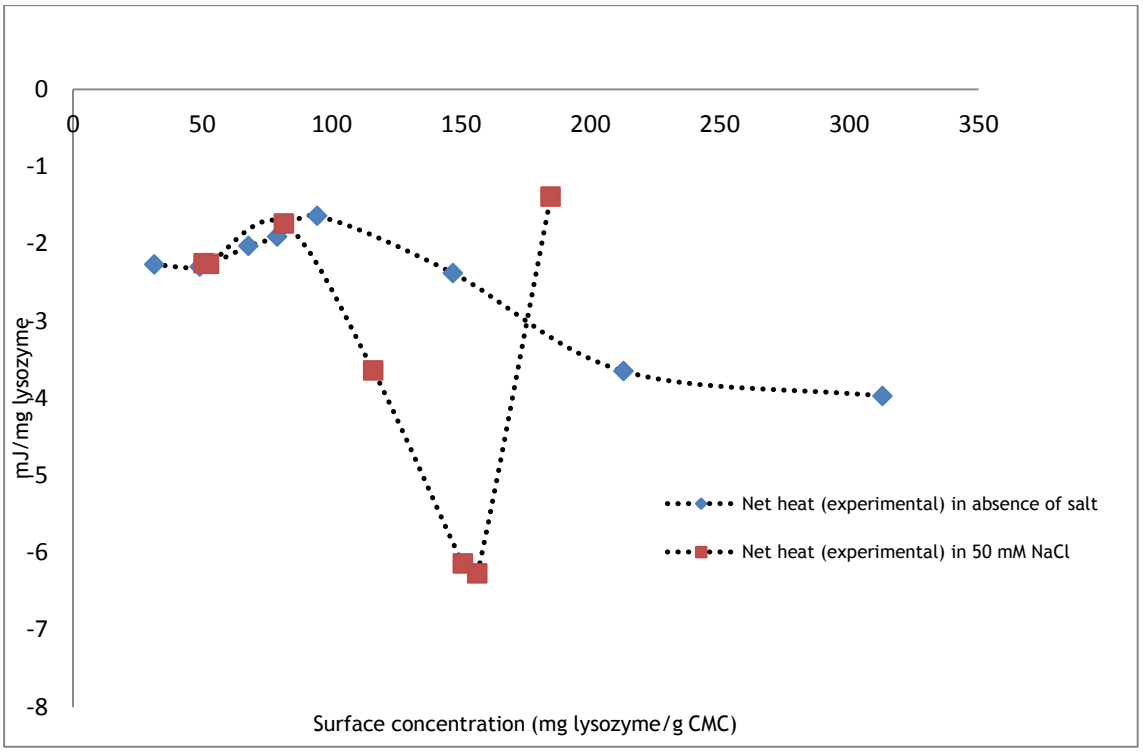

Figure 4.3.22 - Microcalorimetric results of the experimental net heat for the experiments performed with the 30µL loop, with and without salt.

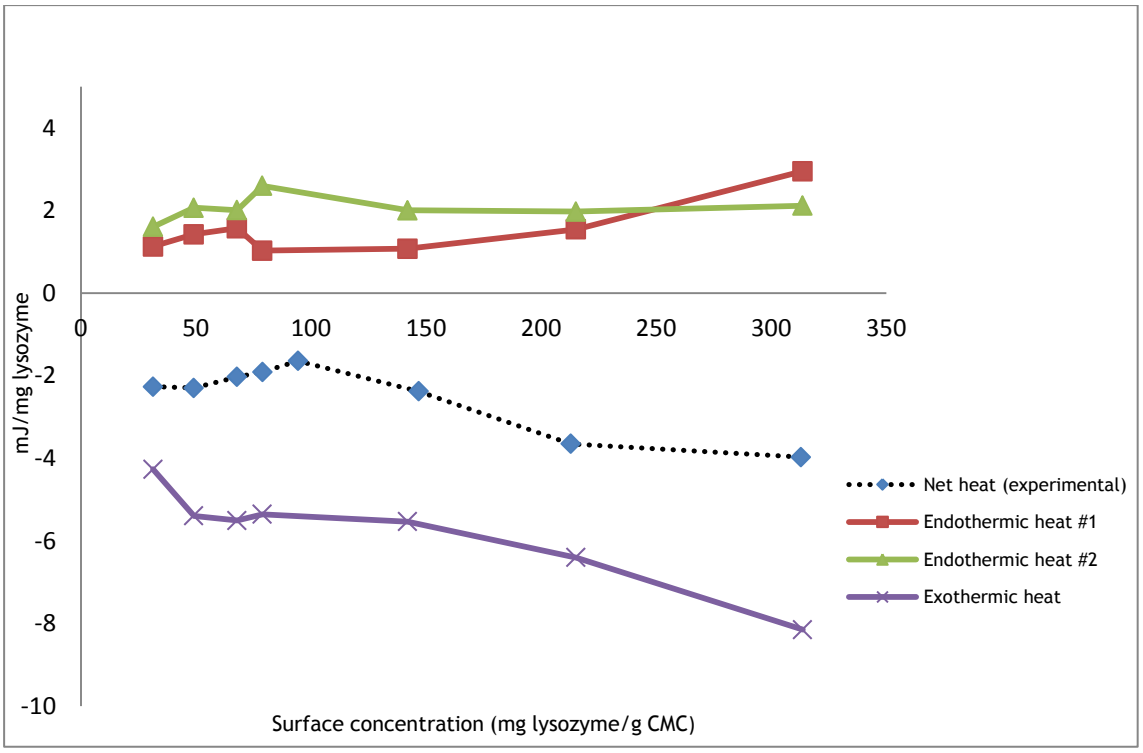

Figure 4.3.23 - Microcalorimetric results of the overall enthalpy for the experiments performed with the 30µL loop without salt.

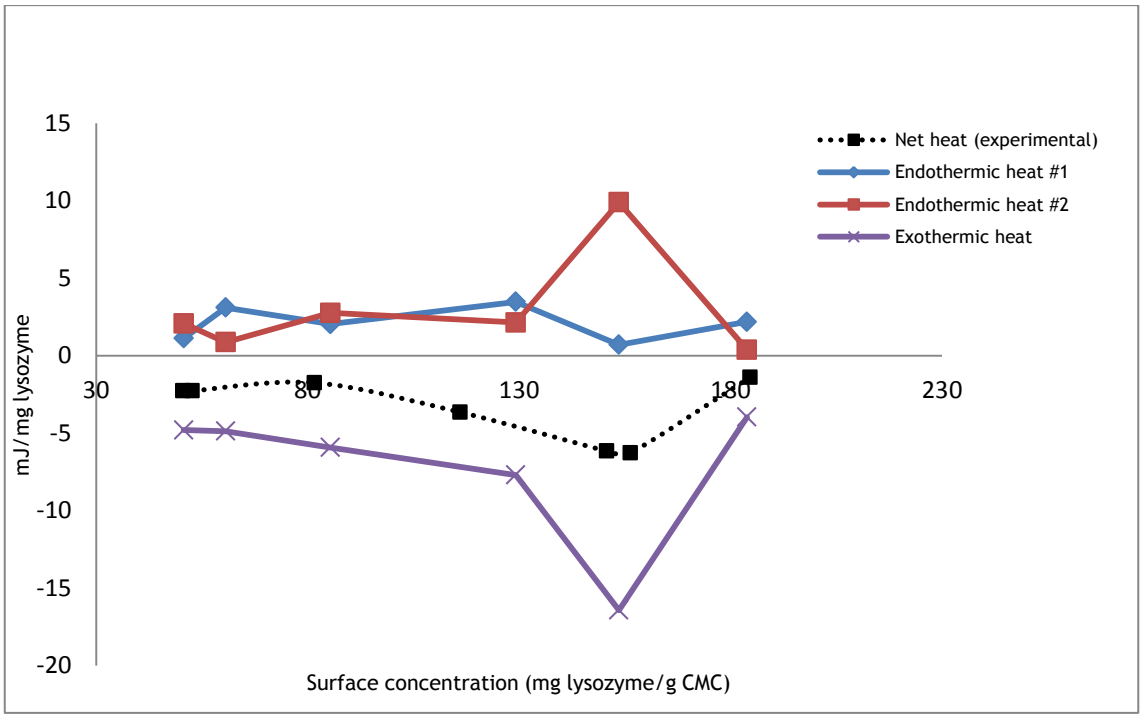

Figure 4.3.24 - Microcalorimetric results of the second endothermic peak for the experiments performed with the 30μL loop with 50mM NaCl.

In the experiments performed at pH 5 in piperazine buffer using the 230μL loop, lysozyme initial concentration varied in the range 40-120mg/mL in the no salted buffer and 20-350mg/mL in the presence of 50mM of NaCl. Figures 4.3.25 and 4.3.26 show the heat signal profile of the injections at the mentioned conditions in the absence of NaCl, resulting in surface concentrations from ~130 to 510mg lysozyme/g CMC. Figure 4.3.29 and 4.3.30 represent the heat signal profile of some of the injections in 50mM NaCl, which resulted in surface concentrations from ~80 to 1100mg lysozyme/g CMC.

Due to the higher protein loading that the longer loop can accommodate, significant differences in the thermogram profile are clear. Therefore, peak de-convolution can give valuable insight about the underlying phenomena in each experiment. The data analysed with MATLAB software is shown after the thermograms. Figures 4.3.27 and 4.3.28 for the no salted injections and 4.3.31-4.3.34 for the presence of 50mM of sodium chloride show the heat signals de-convolution of the experiments with the 230μL.

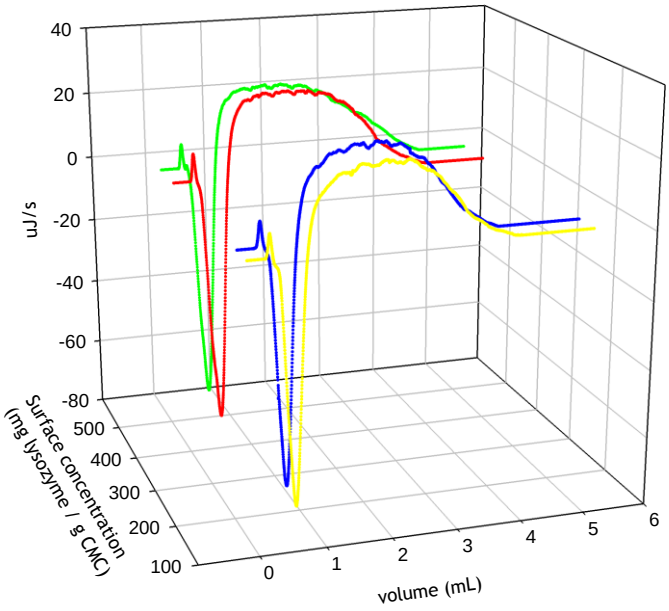

Figure 4.3.25 - Thermograms of lysozyme adsorption on carboxy-methyl cellulose at pH 5 in piperazine buffer 20mM in the absence of salt using a loop of 230µL; Yellow – 130,7mg lysozyme/g CMC; Blue – 169,4mg/g; Red – 450,2mg/g; Green - 513,6mg/g.

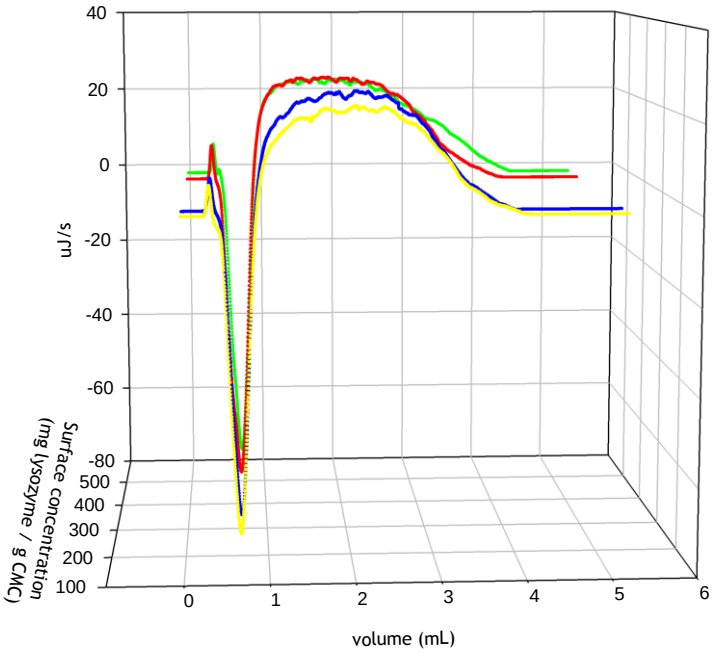

Figure 4.3.26 - Different perspective of the thermograms of lysozyme adsorption on carboxy-methyl cellulose at pH 5 in piperazine buffer 20mM in the absence of salt using a loop of 230µL.

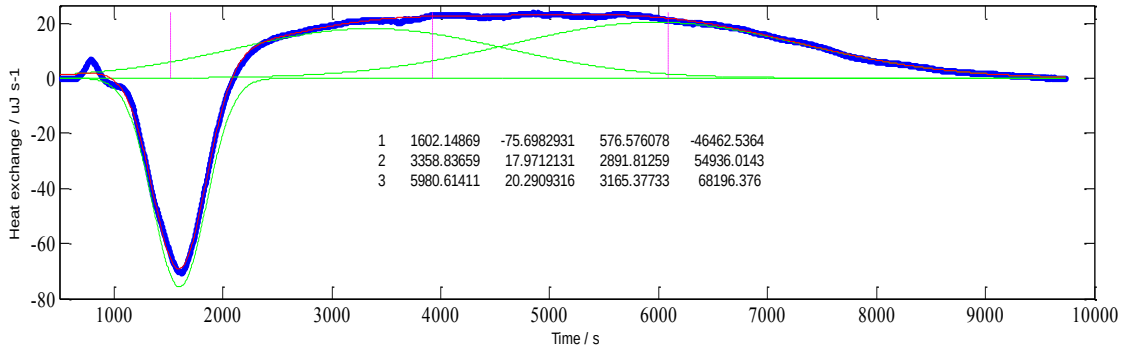

Figure 4.3.27 - MATLAB de-convolution of the thermograms of lysozyme adsorption on carboxy-methyl cellulose at pH 5 in piperazine buffer 20mM using a loop of 230µL. Surface concentration: 130,7mg/g.

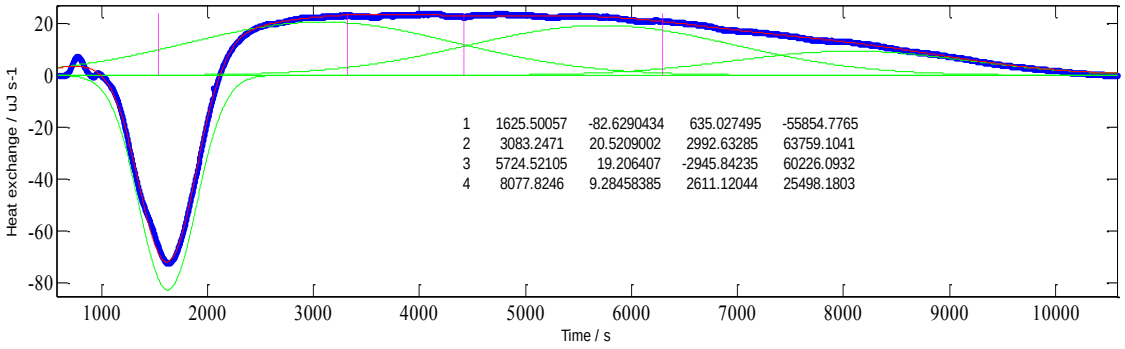

Figure 4.3.28 - MATLAB de-convolution of the thermograms of lysozyme adsorption on carboxy-methyl cellulose at pH 5 in piperazine buffer 20mM using a loop of 230µL. Surface concentration: 513,6mg/g

It is seen that, as with the lower loop, the same distinct events are present, but somehow in a different extension. The first exothermic peak and the endothermic events appear to be energetically stronger. Also, overlapping exothermic peaks show higher complexity than the previous ones. Apart from differences in the protein loadings, the experiments run with the 230µL loop had another key feature: the residence time. Therefore, it is predictable the presence of subsequent adsorption processes, resulting in overlapping exothermic interactions, as seen in the figures for the higher surface concentrations. As protein surface concentration is higher and lysozyme stays in the system longer than in the 30µL injections, is given more time for equilibrium establishment, molecules have more time to reorient and more lysozyme is accommodated resulting in multiple adsorption exothermic peaks.

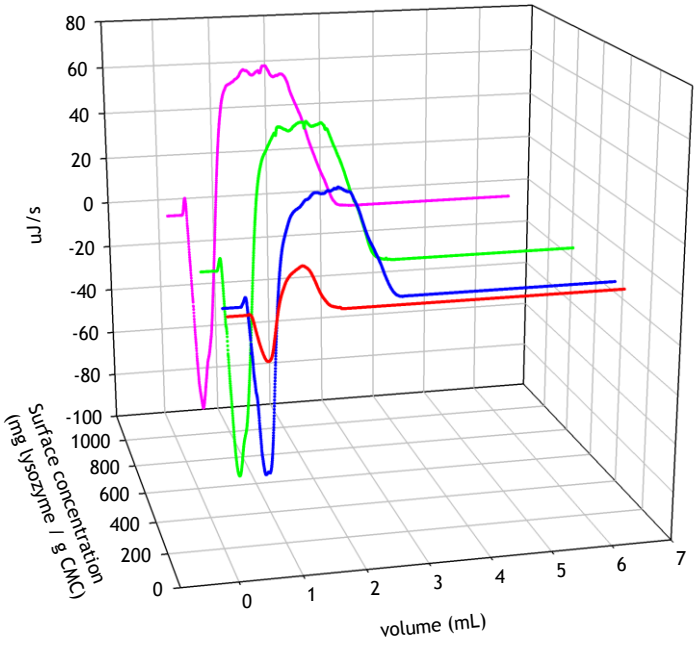

Figure 4.3.29 - Thermograms of lysozyme adsorption on carboxy-methyl cellulose at pH 5 with 50mM NaCl in Piperazine buffer 20mM using a loop of 230µL; Red – 80,5mg lysozyme/g CMC; Blue – 146,4mg/g; Green – 459,7mg/g; Pink – 1018,3mg/g.

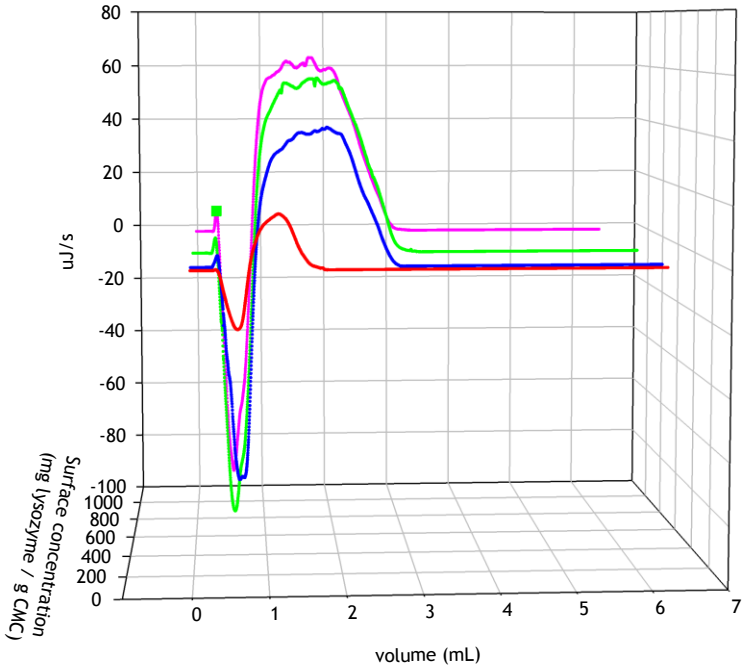

Figure 4.3.30 - Different perspective of the thermograms of lysozyme adsorption on carboxy-methyl cellulose at pH 5 with 50mM NaCl in Piperazine buffer 20mM using a loop of 230µL.

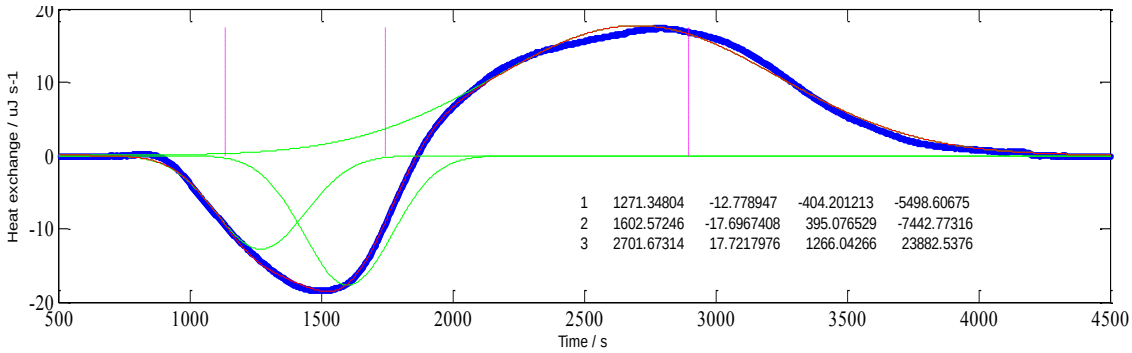

Figure 4.3.31 - MATLAB de-convolution of the thermograms of lysozyme adsorption on carboxy-methyl cellulose at pH 5 with 50mM NaCl in piperazine buffer 20mM using a loop of 230µL. Surface concentration: 80,5mg/g

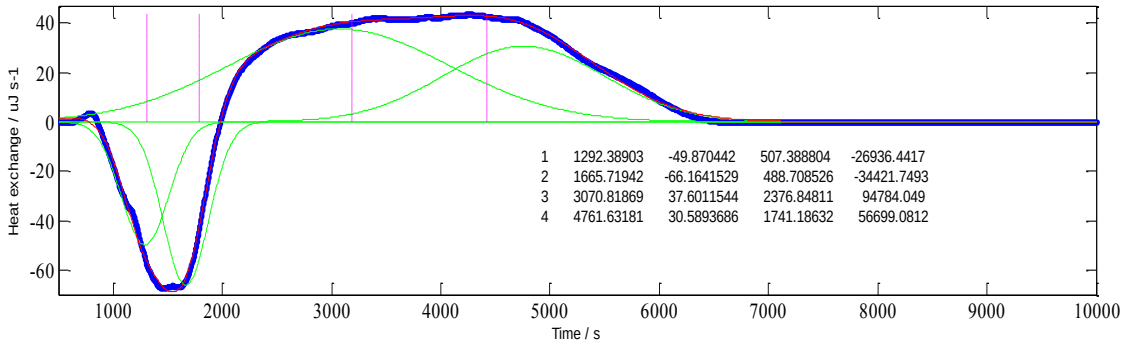

Figure 4.3.32 - MATLAB de-convolution of the thermograms of lysozyme adsorption on carboxy-methyl cellulose at pH 5 with 50mM NaCl in piperazine buffer 20mM using a loop of 230µL. Surface concentration: 146,4mg/g

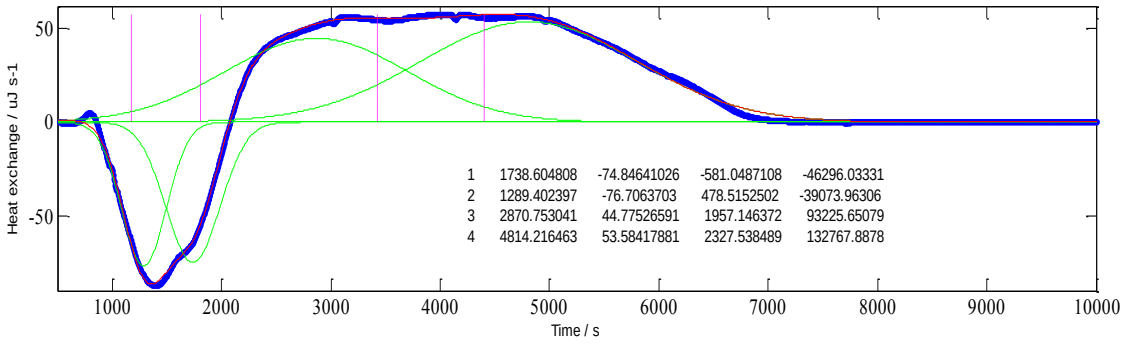

Figure 4.3.33 - MATLAB de-convolution of the thermograms of lysozyme adsorption on carboxy-methyl cellulose at pH 5 with 50mM NaCl in piperazine buffer 20mM using a loop of 230µL. Surface concentration: 459,7mg/g

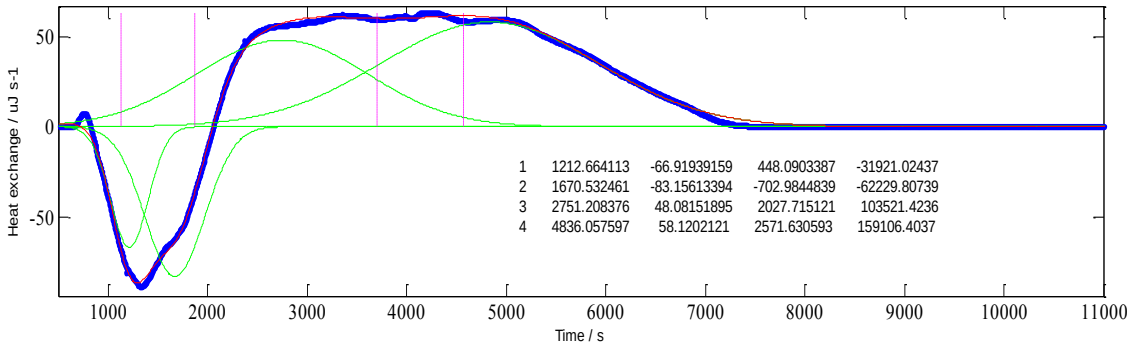

Figure 4.3.34 - MATLAB de-convolution of the thermograms of lysozyme adsorption on carboxy-methyl cellulose at pH 5 with 50mM NaCl in piperazine buffer 20mM using a loop of 230µL. Surface concentration: 1018,3mg/g

In Figure 4.3.35 are displayed, in the same graph, the heat signals of the injections performed with the two different loops used. We chose to show two injections that resulted in approximate surface lysozyme concentration. The blue line show an injection of 90mg/mL in the 30µL loop and the red one represents an injection of 20mg/mL in the 230µL loop. Although the same surface concentration was reached, there were significant differences in the magnitude of reaction's enthalpy, in the duration of the whole interaction and in the time at which each event took place. The plausible explanation for these evidences is, as said before, the residence time of the protein bulk solution inside the cell. Under these circumstances is given more time for equilibrium establishment and the profile of heat exchange becomes better defined. This observation may rise a question, is the neat heat evolution profile as function of surface equilibrium concentration influenced by time of contact between the prove and the adsorbent? To answer this question neat heat evolution as function of surface equilibrium, in the presence of salt, for the two loops has been compared (Figures 4.3.24 and 4.3.36). It is observed that the same profile is present. In both, there is a maximum at approximately the same surface concentration that matches with the point in the isotherm where the curve starts to level. Although the exchanged energy is greater when the 230 ul loop is used, expected because of the greater time leaved for biomolecule – support interaction, the evolution profile is not affected.

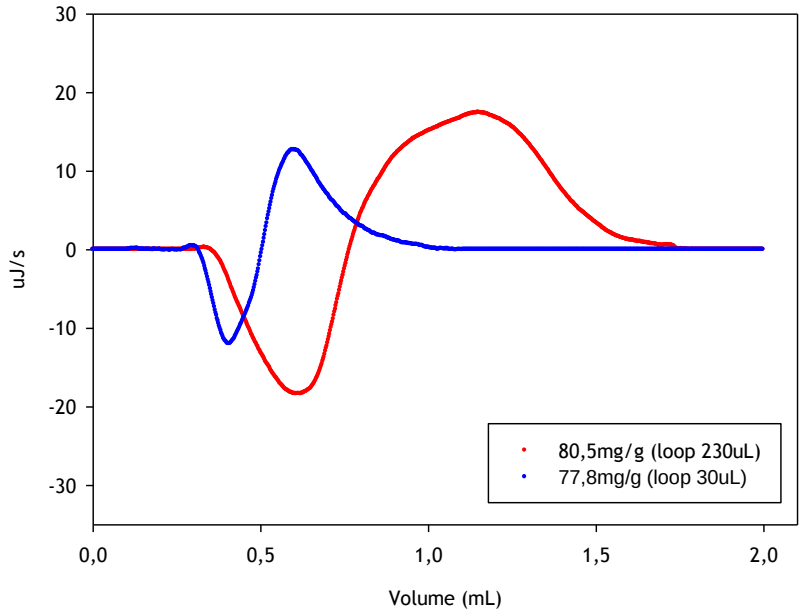

Figure 4.3.35 - Overlapping of an injection of 90mg/mL in the 30µL loop with one of 20mg/mL in the 230µL loop resulting in the same surface concentration.

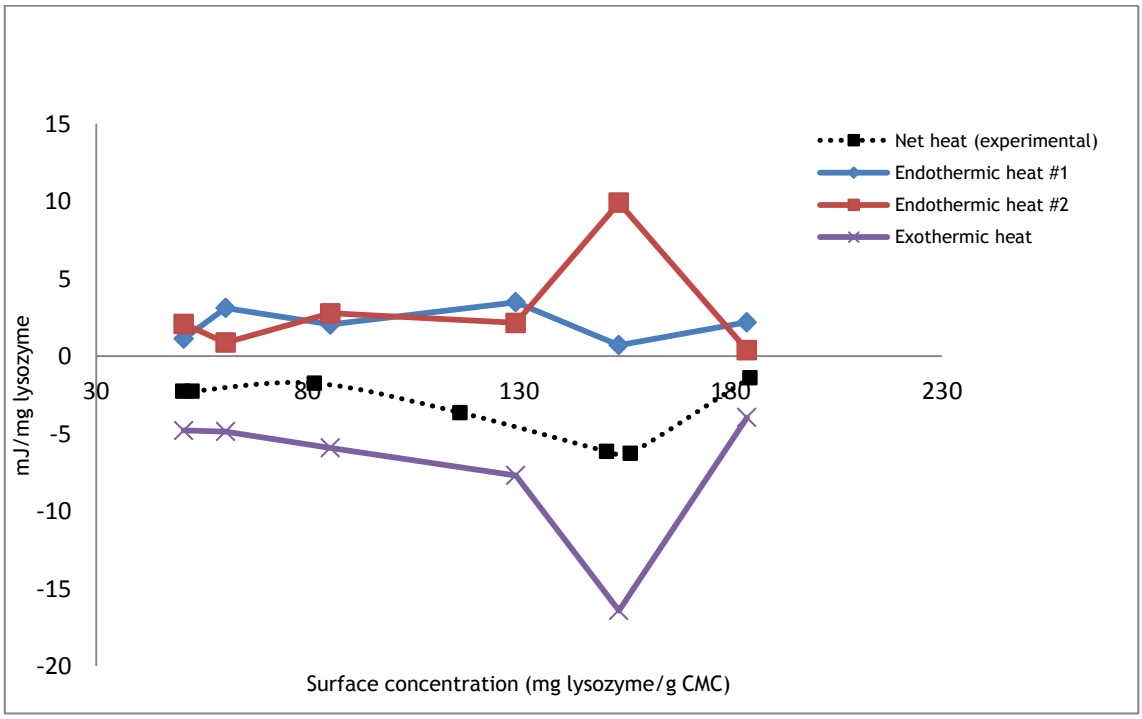

Figure 4.3.24 - Microcalorimetric results of the second endothermic peak for the experiments performed with the 30µL loop with 50mM NaCl (**presented again for simple comparison**).

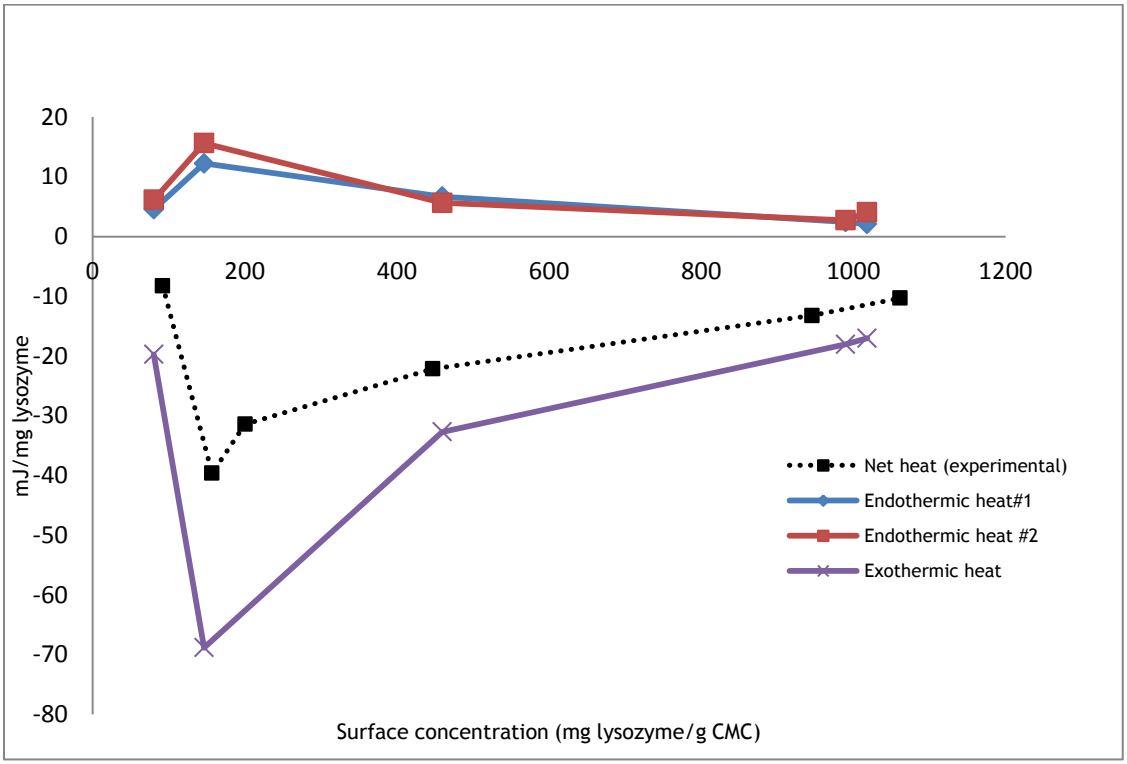

Figure 4.3.36 - Microcalorimetric results of the second endothermic peak for the experiments performed with the 230µL loop with 50mM NaCl.

One of work objectives was the study of adsorption under overloaded conditions; these where achieved in presence of salt and by using the 230µl loop (Figure 4.3.29 and 4.3.30). Observed heat signals, as discussed, show a more complicate profile. The endothermic peak is clearly divided into two peaks and several peaks comprise the exothermic signal. This is not strange, once under non-linear conditions more non-specific effects take place, resulting in less energetic reactions despite the increasing protein surface concentration. In fact, there is a decrease in the exothermic net heat as surface concentration increases under these loading conditions (Figure 4.3.36), despite increasing surface concentration; an explanation for this behaviour may be related with multi-layer formation.

CALDOS software allows measuring not only the heat exchange of the process, ie. Interaction enthalpy, but also detects the protein that is being eluted with a UV system coupled to the microcalorimeter. This gives valuable information about what is happening inside the cell.

Figures 4.3.37-4.3.40 show an overlapping of the heat signal (red) with the UV data (blue) recorded by CALDOS software, of some selected experiments, both in absence and in presence of sodium chloride, run with the loop of 30µL. For each salt condition two experiments are shown: 40mg/mL and 90mg/mL lysozyme injection for the non-salted buffer and 50mg/mL and 200mg/mL injections in the presence of salt.

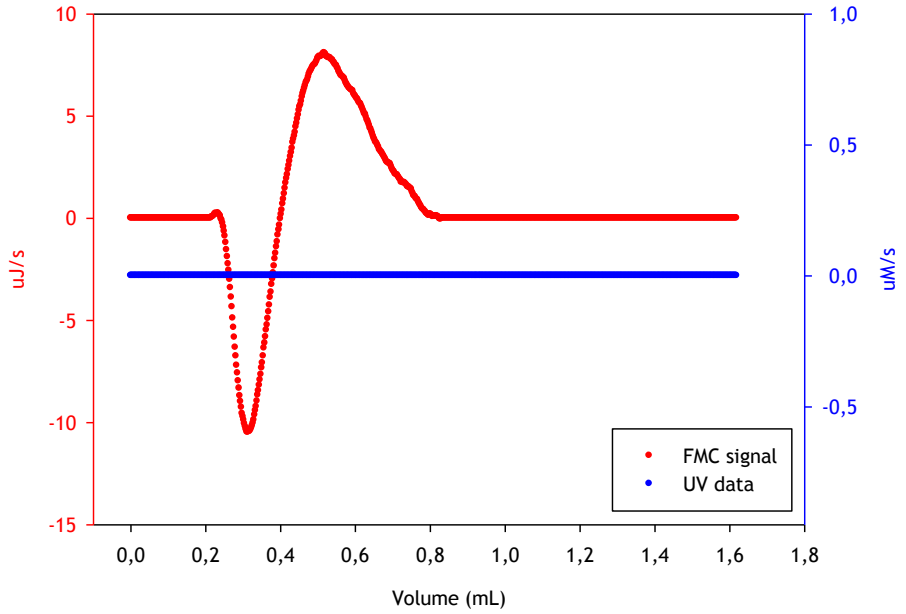

Figure 4.3.37 – Overlapping of FMC and UV signals; Surface concentration: 67,9 mg lysozyme / g CMC; Buffer: Piperazine 20mM at pH 5; loop: 30µL.

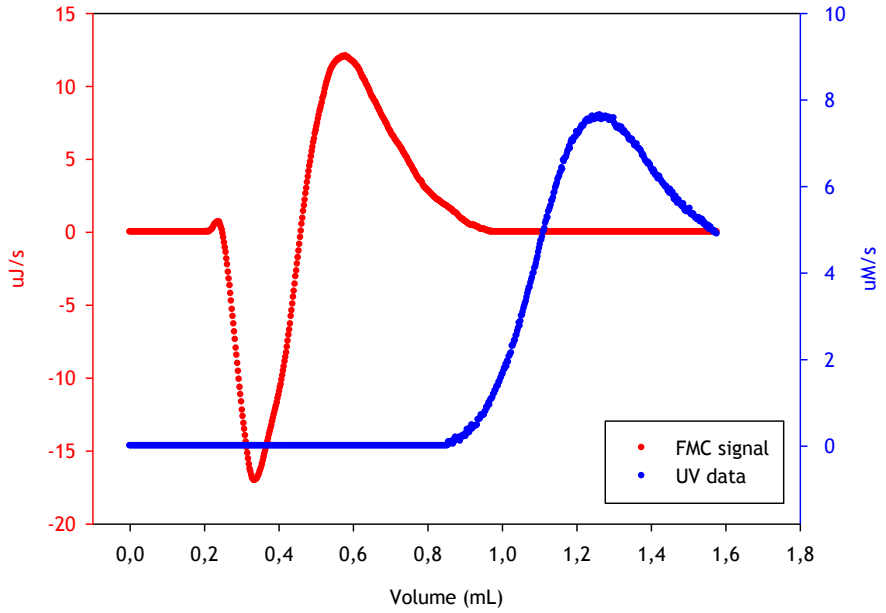

Figure 4.3.38 – Overlapping of FMC and UV signals; Surface concentration: 144,5 mg lysozyme / g CMC; Buffer: Piperazine 20mM at pH 5; loop: 30µL.

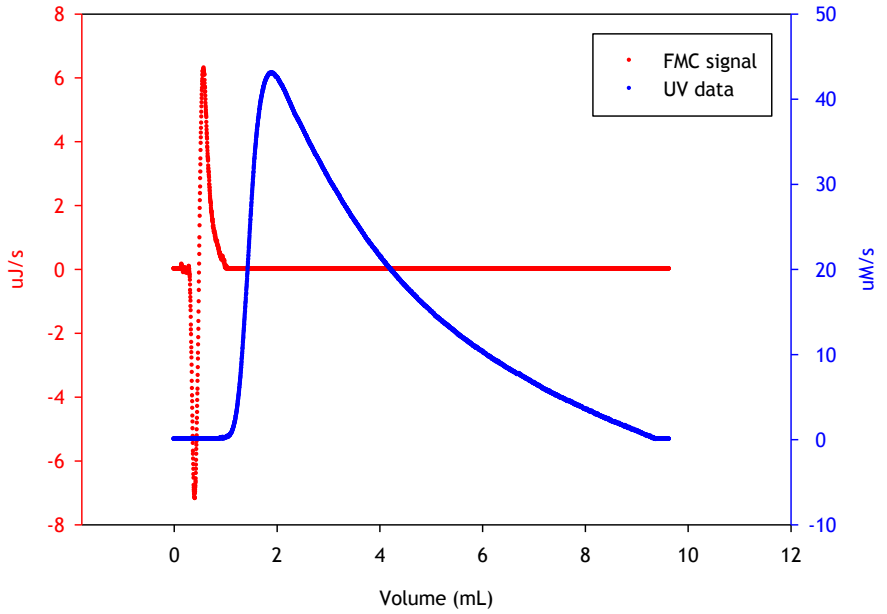

Figure 4.3.39 - Overlapping of FMC and UV signals; Surface concentration: 60,6 mg lysozyme / g CMC; Buffer: Piperazine 20mM + NaCl 50mM at pH 5; loop: 30µL.

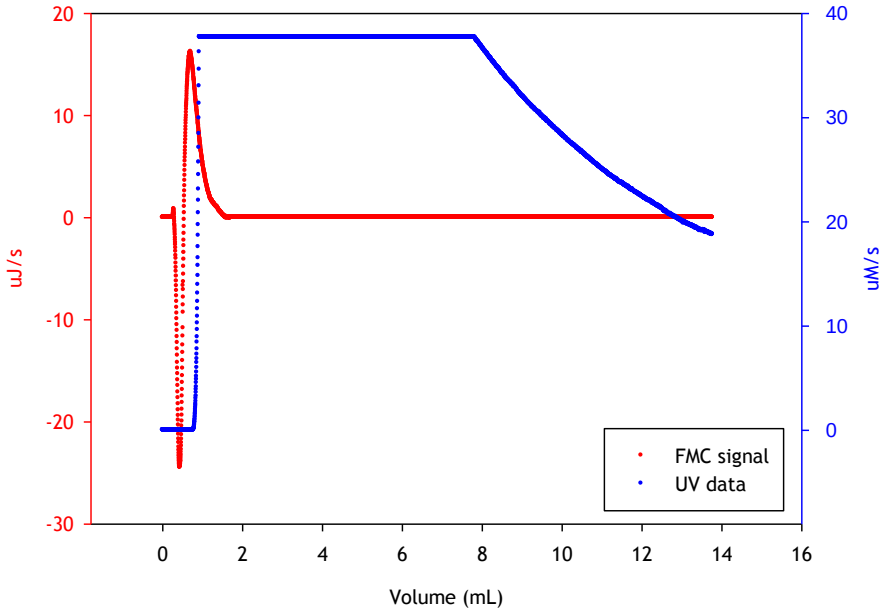

Figure 4.3.40 - Overlapping of FMC and UV signals; Surface concentration: 116,1 mg lysozyme / g CMC; Buffer: Piperazine 20mM + NaCl 50mM at pH 5; loop: 30µL.

In absence of salt, in the experiment of the lowest protein surface concentration, the UV system did not detect any protein coming out of the FMC system. One can only conclude that every protein stayed adsorbed in the CMC, being this consistent with an ion exchange mechanism: strong resin, low protein concentration, no salt, therefore high binding capacity. In the other experiment with no salt (144,5mg/g) (Figure 4.3.38), some protein elutes from the system. However, protein elution only occurs after every interaction within the microcalorimeter had taken place. This has a similar profile to the first graphic for an injection in the presence of salt (Figure 4.3.39). In the second experiment with salt, the protein loading was 200mg lys/g, resulting in 116,1mg of lysozyme adsorbed in each gram of CMC. However, here the protein that does not adsorb starts to be detected where adsorption is still occurring for some lysozyme molecules. This can be explained with the fact that in this experiment a higher protein concentration was injected, saturating the resin surface and pores easily, thus inhibiting other molecules to interact with the adsorbent.

Figures 4.3.41-4.3.44 show the overlapping of the heat signal (red) with the UV data (blue) recorded by CALDOS software of some selected experiments, both in absence and in presence of sodium chloride, run with the loop of 230µL. For each salt condition two experiments are also shown: 40mg/mL and 220mg/mL lysozyme injection for the non-salted buffer and 250mg/mL and 300mg/mL injections in the presence of salt.

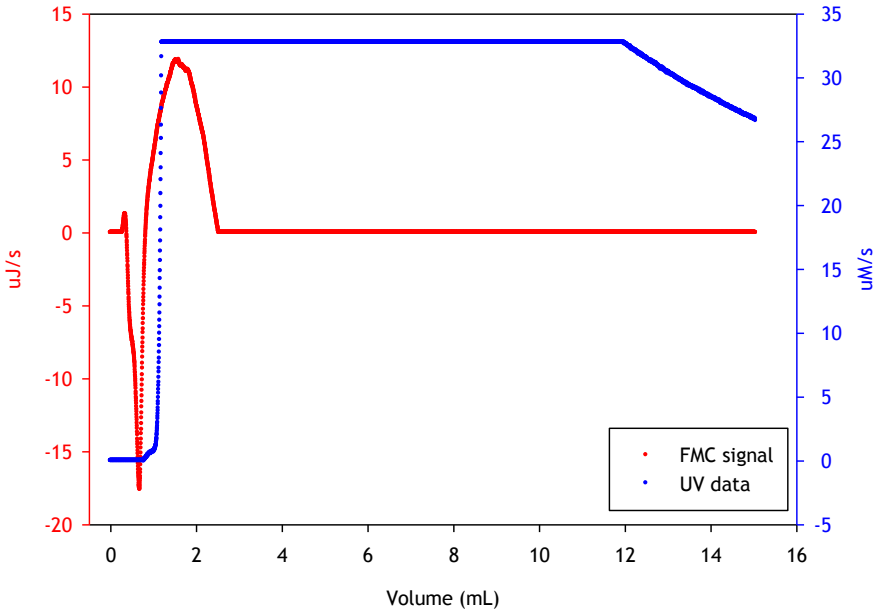

Figure 4.3.41 - Overlapping of FMC and UV signals; Surface concentration: 354,3 mg lysozyme / g CMC; Buffer: Piperazine 20mM at pH 5; loop: 230µL.

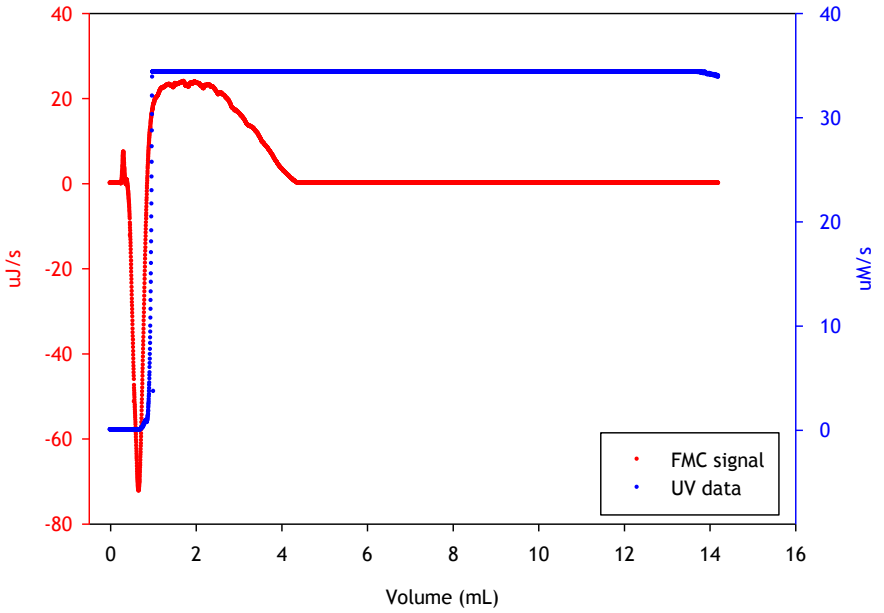

Figure 4.3.42 - Overlapping of FMC and UV signals; Surface concentration: 513,6 mg lysozyme / g CMC; Buffer: Piperazine 20mM at pH 5; loop: 230µL.

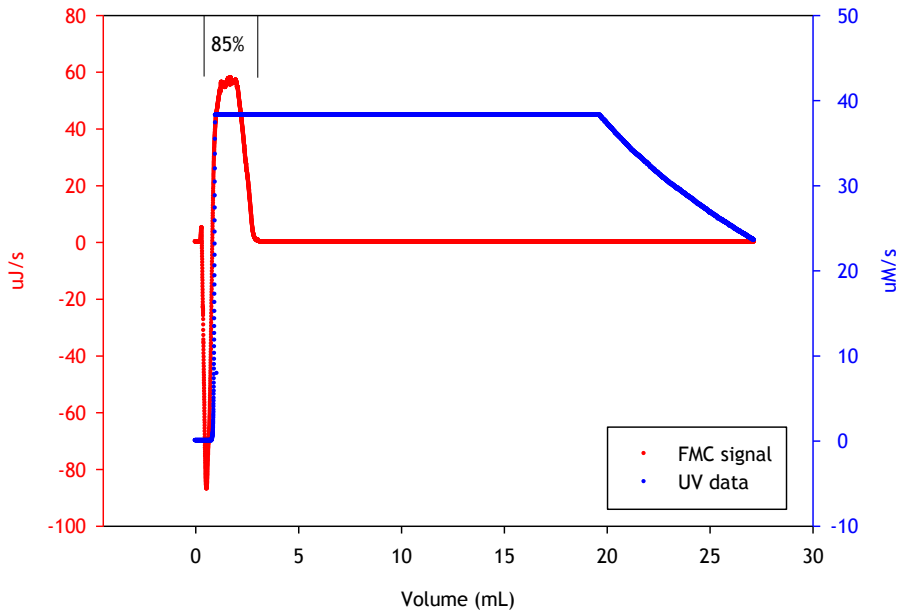

Figure 4.3.43 - Sobreposition of FMC and UV signals; Surface concentration: 459,7 mg lysozyme / g CMC; Buffer: Piperazine 20mM + NaCl 50mM at pH 5; loop: 230µL.

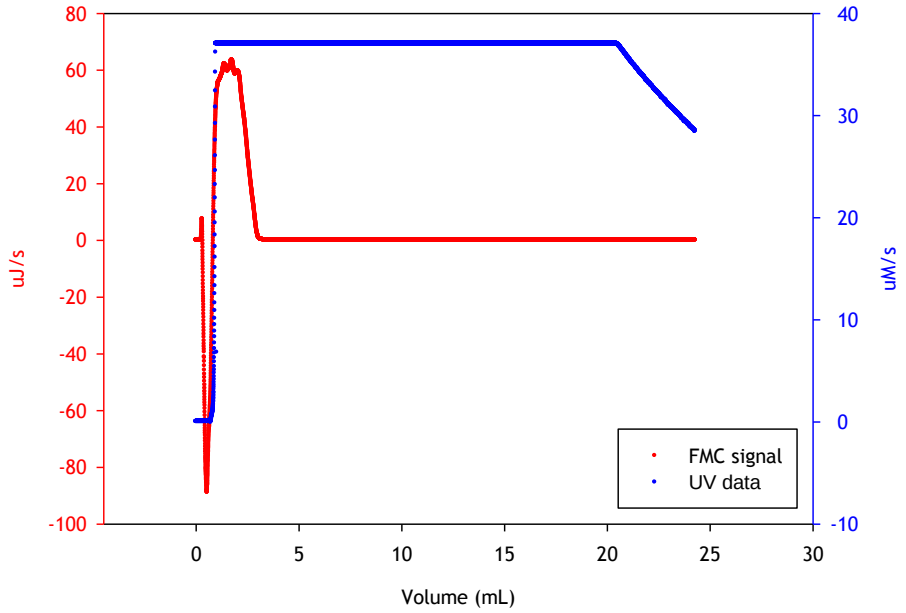

Figure 4.3.44 - Sobreposition of FMC and UV signals; Surface concentration: 1018,3 mg lysozyme / g CMC; Buffer: Piperazine 20mM + NaCl 50mM at pH 5; loop: 230µL.

The FMC cell has a known volume of 171µL, lower than the loop itself, this explains why the UV signal starts to be detected even when there are interactions occurring in the FMC system. In the experiments, performed under overloaded conditions, regardless the loop volume, lysozyme flow starts to be detected by the UV system at approximately the same time. Again, because of oversaturation of the chromatography support, while some protein is still interacting with the adsorbent, the molecules that do not interact are already being detected by UV system. In the experiment in which 250mg/mL of lysozyme were injected (Figure 4.3.43), which resulted in a surface concentration of 459,7mg/g, we collected fractions at different time gaps as protein was eluting. Eight collections were done and the protein concentration was measured in each one. The first six collections lasted until the second hour (3mL) of the experiment, which corresponds to the time where the contact between the probe and the resin packed in the FMC system stopped. By this time, already 85% of the total protein that did not stayed adsorbed had already been collected. The experiment continued to run for about more 16 hours and during this time lapse the remaining 15% of protein eluted. Since during these last 16 hours no apparent changes in overall reaction enthalpy were detected by the thermistors inside the FMC cell but still some protein was eluting, we can only assume that this was an entropic phenomenon caused by protein leaking.

The microcalorimetric studies for BSA adsorption onto Toyopearl GigaCap Q-650M resulted in the graphics showed in Figure 4.3.41 and 4.3.42. In these experiments it was used the injection loop of 230µL and the flow rate was kept constant at 1,5mL/h. As already said in the Experimental section, these injections were performed at pH 8 in tris-HCl buffer 20mM in the absence of salt.

The loading concentrations varied from 10 to 150mg/mL resulting in protein surface concentrations between 165-830mg BSA/g resin.

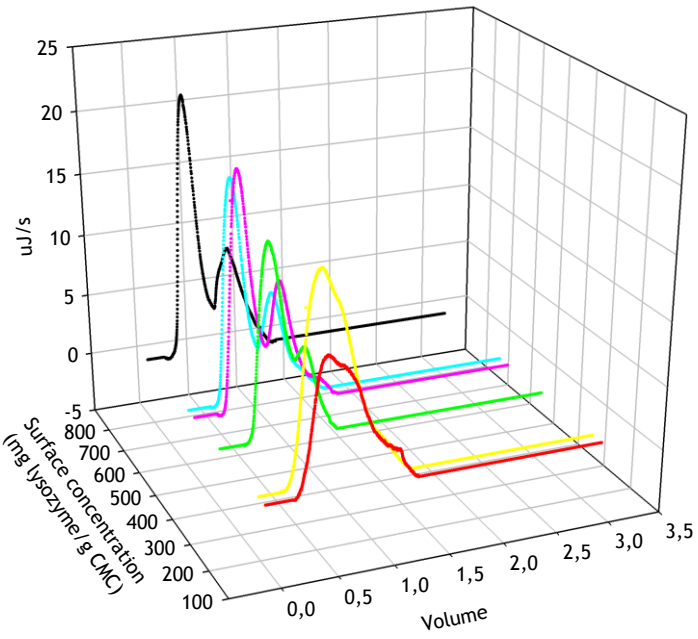

Figure 4.3.41 - Thermograms of BSA adsorption on Toyopearl Giga-Cap Q-650M at pH 8 in tris-HCl buffer 20mM in the absence of salt using a loop with 230µL; Red – 169,1mg lysozyme/g CMC; Yellow – 202,2mg/g; Green – 400,0mg/g; Pink – 540,7mg/g; Cyan – 575,0mg/g; Black – 828,2mg/g.

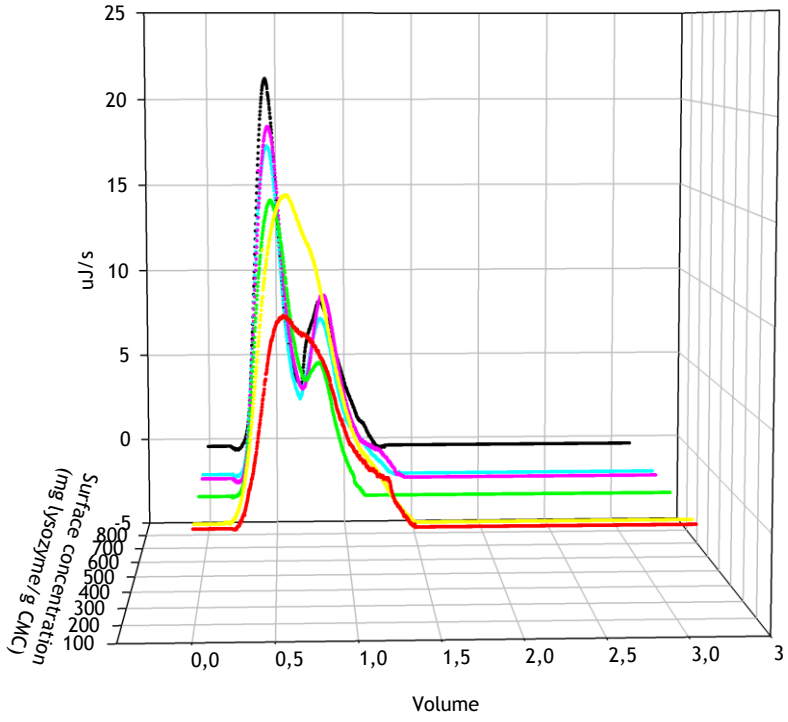

Figure 4.3.42 - Different perspective of the thermograms of BSA adsorption on Toyopearl Giga-Cap Q-650M at pH 8 in tris-HCl buffer 20mM in the absence of salt using a loop with 230µL

As observed from the resulting profile and from signal de-convolution (Figures 4.3.43-4.3.48), resulting heat from BSA adsorption onto GigaCap Q-650M show that overlapping exothermic events are present. GigaCap Q-650M is a polymeric modified resin, allowing a better access to its ligands, making this resin even stronger when compared with other strong anion exchangers. Thanks to microcalorimetric studies, it can be seen that BSA adsorption at surface concentrations between 150-200mg/g, corresponding to the plateau of the isotherm, the reaction is highly exothermic compared to higher surface concentrations (Figures 4.3.49 and 4.3.50). This is an expected result since the binding surface area available to the ligands is decreasing as surface concentration increases.

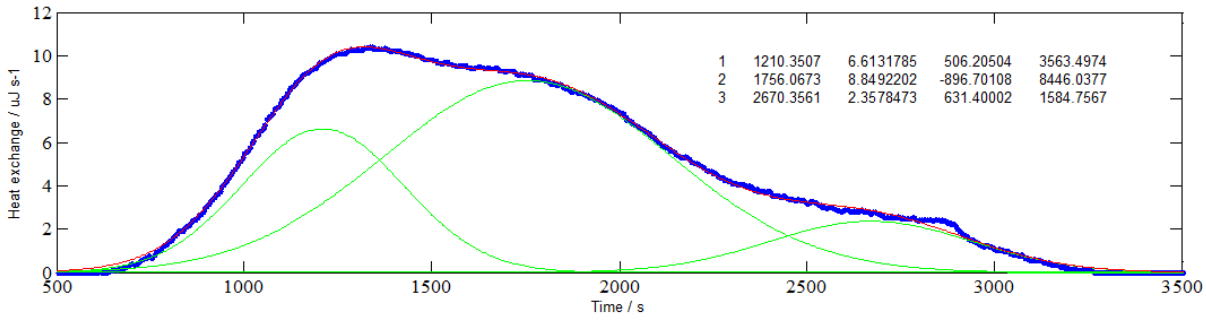

Figure 4.3.43 - MATLAB de-convolution of the thermograms of BSA adsorption on GigaCap Q-650M at pH 8 in tris-HCl buffer 20mM using a loop of 230µL. Surface concentration: 169,1mg/g.

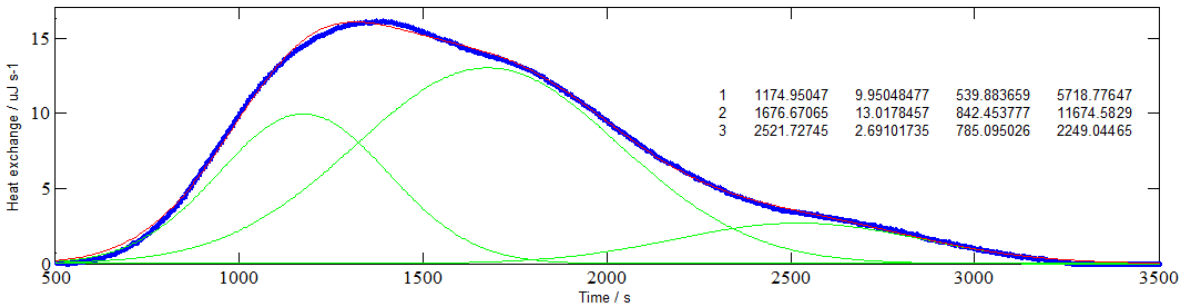

Figure 4.3.44 - MATLAB de-convolution of the thermograms of BSA adsorption on GigaCap Q-650M at pH 8 in tris-HCl buffer 20mM using a loop of 230µL. Surface concentration: 202,2mg/g.

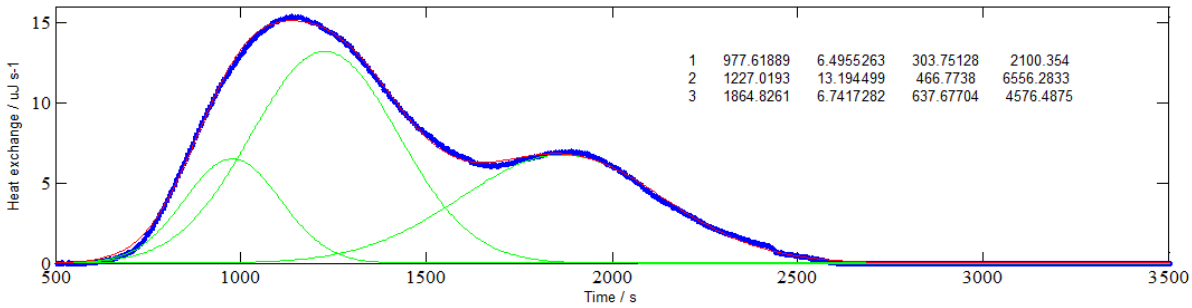

Figure 4.3.45 - MATLAB de-convolution of the thermograms of BSA adsorption on GigaCap Q-650M at pH 8 in tris-HCl buffer 20mM using a loop of 230µL. Surface concentration: 400,0mg/g.

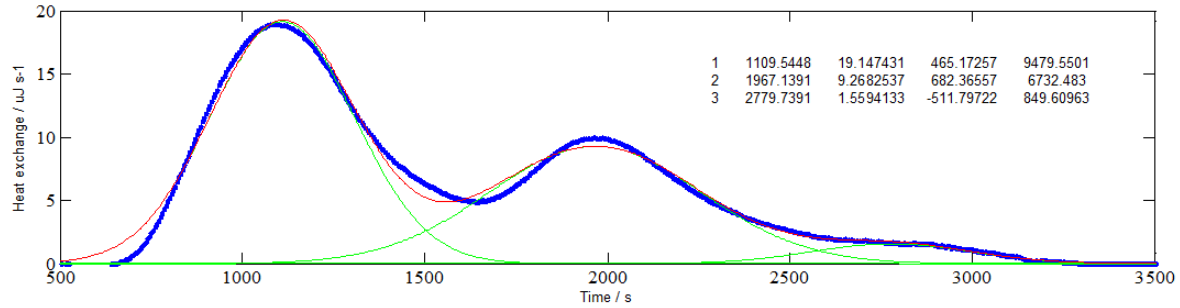

Figure 4.3.46 - MATLAB de-convolution of the thermograms of BSA adsorption on GigaCap Q-650M at pH 8 in tris-HCl buffer 20mM using a loop of 230µL. Surface concentration: 540,7mg/g.

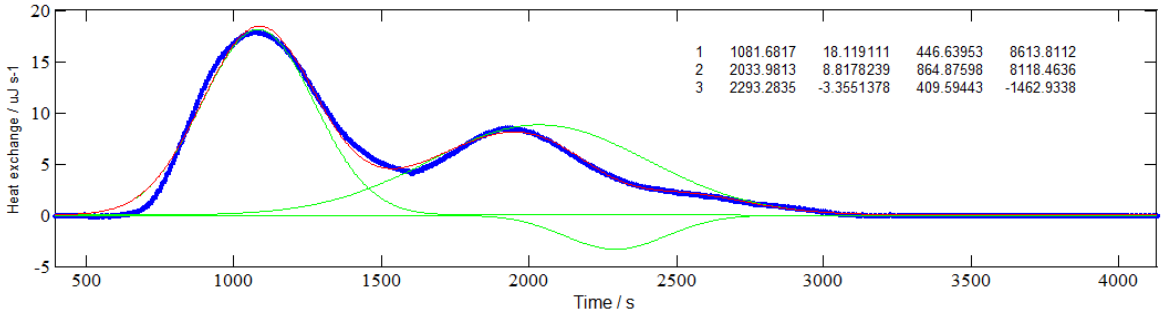

Figure 4.3.47 - MATLAB de-convolution of the thermograms of BSA adsorption on GigaCap Q-650M at pH 8 in tris-HCl buffer 20mM using a loop of 230µL. Surface concentration: 575,0mg/g.

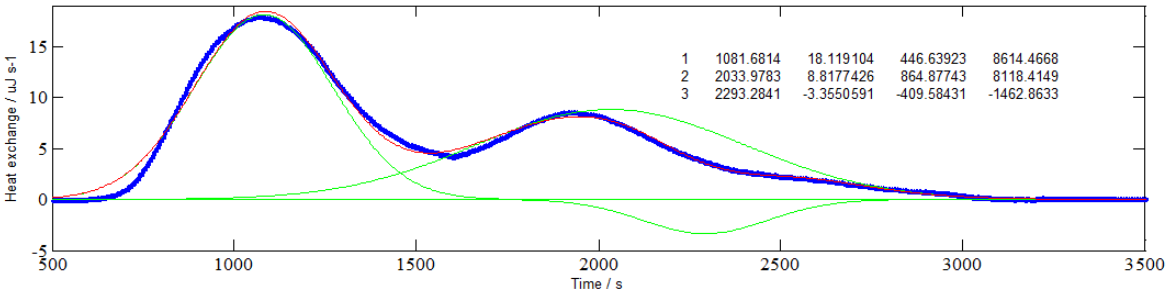

Figure 4.3.48 - MATLAB de-convolution of the thermograms of BSA adsorption on GigaCap Q-650M at pH 8 in tris-HCl buffer 20mM using a loop of 230µL. Surface concentration: 828,2mg/g.

Three exothermic events were observed in each of these tests. The first exotherm may results from attractive protein–surface interactions that mask endothermic influence of surface water molecules and ion release. It is observed that this exotherm is reduced with the increase in loading; this may be due to the rise in repulsive interactions between the adsorbed protein molecules.

The second exothermic peaks are start to appear after the end of the loaded protein bulk solution elutes, considering that we have used a flow rate of 1,5 ml/h and the cell has a volume of 171µl. This timing indicates that the second exotherm is not the result of the formation of secondary adsorbed layers. This is consistent with the adsorption isotherm (Figure 4.1.5). Instead, this second peak can be attributed to the secondary adsorption of BSA molecules due to alteration of conformation, since this biomolecule is considered to be soft [65]. After the primary BSA adsorption on the GigaCap surface, the BSA molecules undergo conformational changes that create new sites on the protein surface which are available for favourable interactions with the adsorption surface. This conclusion is supported by the work of Katiyar et al. [46]. Also, the magnitude of enthalpy decreases as BSA loading increases. This trend can be explained by the fact that the protein–surface interactions are stronger at lower protein loadings. These strong interactions are responsible for greater conformational changes, which drive the secondary adsorption process.

Finally, it can be seen that in the range 575-830mg/g the usual third exothermic heat characteristic of lower concentrations becomes endothermic. Isotherm information in this range would help to understand this behaviour. Nevertheless, at these surface concentrations it is expected repulsion between adsorbed molecules, causing also endothermic heats.

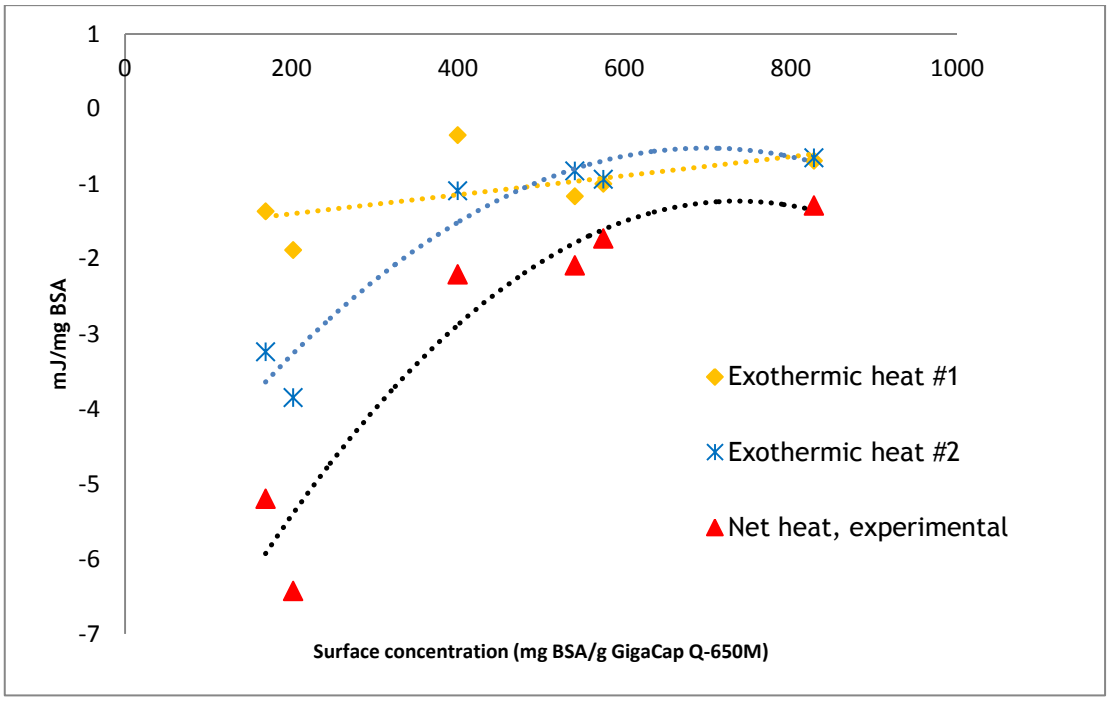

Figure 4.3.49 - Microcalorimetric results of the first exothermic peaks and experimental net heat for BSA adsorption onto GigaCap Q-650M performed with the 230µL loop.

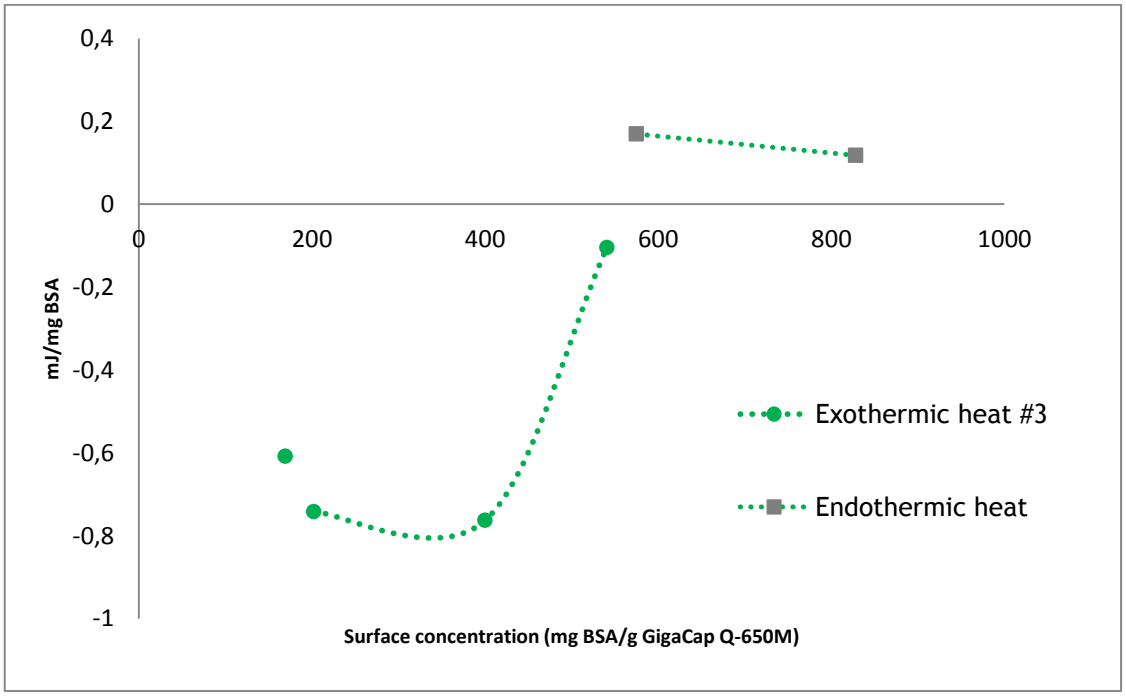

Figure 4.3.50 - Microcalorimetric results of the third exothermic peak and endothermic heat for BSA adsorption onto GigaCap Q-650M performed with the 230µL loop.

Chapter V – Conclusions and future work

This dissertation had the objective of studying the adsorption mechanisms underlying ion-exchange chromatography. Since adsorption is a phenomenon were energy changes are associated, microcalorimetry was used and gave valuable insight on the overall process.

Firstly, lysozyme adsorption mechanism onto CMC was studied at pH 5 both in absence and in presence of sodium chloride (50mM). It was seen that under linear protein concentrations the exothermic net heats are similar for both salt conditions, indicating that when the chromatographic resin still has empty binding sites lysozyme adsorbs freely regardless salt concentration. However, when surface concentration reached the point where the isotherm starts to level, an increase in the endothermic heat is seen in the presence of salt. At these surface protein concentrations, lysozyme "feels" an extra urge to reorient in order to try to accommodate more molecules. This reorientation is favoured in the presence of salt because of the screening effect to the protein charge. Reorientation of lysozyme then leads to a secondary adsorption, which is consistent with the results that show a high exothermic net heat at these protein concentrations. Under overloaded conditions in the presence of salt, with increasing surface concentration, it is seen that there is a decrease in the net heat signal. This is expected since after reorientation there is an energetic equilibrium towards the formation of a new layer and multilayer formation may be present.

Anion-exchange studies with BSA and a grafted resin (Toyopearl GigaCap Q-650M) showed highly exothermic interactions, where three exotherms were present. It was observed that with increase in protein surface concentration, the first exothermic heat decreases, consistent with repulsive interactions between adsorbed molecules. The second exothermic peak seems to be caused by protein secondary adsorption due to alteration of conformation of BSA. Finally, at low protein concentrations a typical third exothermic heat is present. However, at higher surface concentrations there is an endothermic peak instead, probably due to high protein repulsion.

All of these results confirmed that for a more consistent overview of ion-exchange interaction mechanism, flow microcalorimetry could be of great interest in a systematic study.

The future work perspective is to conclude the investigation of the underlying mechanisms of lysozyme adsorption onto CMC. It is intended to further extend the research to overloaded protein concentrations in the absence of salt. Also, doing some experiments under a higher ionic strength would help to understand better how salt concentration affects protein adsorption. In addition, protein charge is one of the most important factors in ion-exchange, so, changing the pH would give valuable insight into the overall process.

Last but not least, it is intended to keep reseach by microcalorimetry for Toyopearl® resins (GigaCap Q-650M and DEAE-650M) in order to understand how the polymeric modification of the resin particle affects protein binding.

References

[1] M. Hedhammar, A.E. Karlström, S. Hober, Chromatographic methods for protein purification, Royal Institute of Technology, Stockholm, Sweden.

[2] M.E. Thrash Jr, J.M. Phillips, N.G. Pinto, Adsorption. 10 (2005) 299–307.

[3] A. Staby, I.H. Jensen, I. Mollerup, Journal of Chromatography A. 897 (2000) 99–111.

[4] A. Staby, I.H. Jensen, Journal of Chromatography A. 908 (2001) 149–161.

[5] A. Staby, M.-B. Sand, R.G. Hansen, J.H. Jacobsen, L. A. Andersen, M. Gerstenberg, et al., Journal of Chromatography A. 1034 (2004) 85–97.

[6] A. Staby, M.-B. Sand, R.G. Hansen, J.H. Jacobsen, L. A. Andersen, M. Gerstenberg, et al., Journal of Chromatography A. 1069 (2005) 65–77.

[7] A. Staby, J.H. Jacobsen, R.G. Hansen, U.K. Bruus, I.H. Jensen, Journal of Chromatography A. 1118 (2006) 168–79.

[8] A. Staby, R.H. Jensen, M. Bensch, J. Hubbuch, D.L. Dünweber, J. Krarup, et al., Journal of Chromatography A. 1164 (2007) 82–94.

[9] M.E. Thrash Jr, N.G. Pinto, Journal of Chromatography A. 944 (2002) 61–68.

[10] E. Müller, Chemical Engineering & Technology. 28 (2005) 1295–1305.

[11] TOSOH Bioscience, Chromatographic Process Media Catalog.

[12] J. Korfhagen, A.C. Dias-Cabral, M.E. Thrash Jr, Separation Science and Technology. 45 (2010) 2039–2050.

[13] P. Raje, N.G. Pinto, Journal of Chromatography A. 760 (1997) 89–103.

[14] P. Raje, N.G. Pinto, Journal of Chromatography A. 796 (1998) 141–56.

[15] M.E. Thrash Jr, N.G. Pinto, Journal of Chromatography A. 1126 (2006) 304–10.

[16] S. Yamamoto, K. Nakanishi, R. Matsuno, Ion Exchange Chromatography of Proteins, Taylor & Francis, 1988.

[17] TOSOH Bioscience, General Principles of Liquid Chromatography.

[18] A.K. Hunter, G. Carta, Journal of Chromatography A. 897 (2000) 65–80.

[19] F.G. Helfferich, Ion Exchange, Courier Dover Publications, 1962.

[20] J. Ståhlberg, Journal of Chromatography. A. 855 (1999) 3–55.

[21] E. Müller, Journal of Chromatography A. 1006 (2003) 229–240.

[22] L.E. Weaver, G. Carta, Biotechnology Progress. 12 (1996) 342–355.

[23] C. Chang, A.M. Lenhoff, Journal of Chromatography A. 827 (1998) 281–93.

[24] J.J. Van Deemter, F.J. Zuiderweg, A. Klinkenber, Chemical Engineering. 5 (1956) 271–289.

[25] J.C. Bellot, J.S. Condoret, Process Biochemistry. 28 (1993) 365–376.

[26] I. Langmuir, Journal of the American Chemical Society. 40 (1918) 1361–1403.

[27] F.G. Helfferich, P.W. Carr, Journal of Chromatography. 629 (1993) 97–122.

[28] S.R. Gallant, A. Kundu, S.M. Cramer, Journal of Chromatography A. 702 (1995) 125–142.

[29] P.K. de Bokx, P.C. Baarslag, H.P. Urbach, Journal of Chromatography. 594 (1992) 9–22.

[30] P. Jandera, G. Guiochon, Journal of Chromatography A. 605 (1992) 1–17.

[31] W. Kopaciewicz, M.A. Rounds, J. Fausnaugh, F.E. Regnier, Journal of Chromatography. 266 (1983) 3–20.

[32] M.A. Rounds, F.E. Regnier, Journal of Chromatography. 283 (1984) 37–45.

[33] F.E. Regnier, I. Mazsaroff, Biotechnology Progress. 3 (1987) 22–26.

[34] A. Velayudhan, C. Horvath, Journal of Chromatography. 443 (1988) 13–29.

[35] W. Kopaciewicz, M.A. Rounds, F.E. Regnier, Journal of Chromatography. 318 (1985) 157–172.

[36] W.-Y. Chen, Z.-C. Liu, P.-H. Lin, C.-I. Fang, S. Yamamoto, Separation and Purification Technology. 54 (2007) 212–219.

[37] C.A. Brooks, S.M. Cramer, AIChE Journal. 38 (1992) 1969–1978.

[38] Y. Li, N.G. Pinto, Journal of Chromatography A. 702 (1995) 113–123.

[39] M.R. Oberholzer, A.M. Lenhoff, Langmuir. 15 (1999) 3905–3914.

[40] J.C. Bosma, J.A. Wesselingh, AIChE Journal. 50 (2004) 848–853.

[41] G. Carta, Biotechnology Journal. 7 (2012) 1216–20.

[42] C.M. Roth, K.K. Ungerb, A.M. Lenhoff, Journal of Chromatography A. 726 (1996) 45–56.

[43] C. Harinarayan, J. Mueller, A. Ljunglo, R. Fahrner, Biotechnology and Bioengineering. (2006) 775–787.

[44] A.M. Hardin, C. Harinarayan, G. Malmquist, A. Axén, R. van Reis, Journal of Chromatography A. 1216 (2009) 4366–71.

[45] R.A. Alberty, Journal of the American Chemical Society. 91 (1969) 3899–3903.

[46] A. Katiyar, S.W. Thiel, V. V Guliants, N.G. Pinto, Journal of Chromatography A. 1217 (2010) 1583–8.

[47] M.E. Thrash Jr, N.G. Pinto, Journal of Chromatography A. 908 (2001) 293–299.

[48] M. Ornelas, D. Loureiro, M.J. Araújo, E. Marques, C. Dias-Cabral, M. Azenha, et al., Journal of Chromatography A. 1297 (2013) 138–45.

[49] M.A. Esquibel-King, A.C. Dias-Cabral, J.A. Queiroz, N.G. Pinto, Journal of Chromatography A. 865 (1999) 111–122.

[50] A.C. Dias-Cabral, N.G. Pinto, J.A. Queiroz, Separation Science and Technology. 37 (2002) 1505–1520.

[51] D.S. Gill, D.J. Roush, R.C. Willson, Journal of Colloid and Interface Science. 167 (1994) 1–7.

[52] W.R. Bowen, D.T. Hughes, Journal of Colloid and Interface Science. 158 (1993) 395–402.

[53] J.L.M. McNay, J.P.O. Connell, E.J. Fernandez, Biotechnology and Bioengineering. 76 (2001) 233–240.

[54] F.Y. Lin, W.Y. Chen, R.C. Ruaan, H.M. Huang, Journal of Chromatography A. 872 (2000) 37–47.

[55] W.R. Bowen, L.-C. Pan, Journal of Colloid and Interface Science. 189 (1997) 328–336.

[56] M.P. Deutscher, Guide To Protein Purification, in: Methods in Enzymology (1990) 409–413.

[57] W. Norde, Advances in Colloid and Interface Science. 25 (1986) 267–340.

[58] T.P. Perkins, D.S. Mak, T.W. Root, E.N. Lightfoot, Journal of Chromatography A. 766 (1997) 1–14.

[59] F. Xia, D. Nagrath, S.M. Cramer, Journal of Chromatography A. 1079 (2005) 229–235.

[60] TOSOH Bioscience, Toyopearl Instruction Manual.

[61] W. Norde, C.I. Anusiem, Colloids and Surfaces. 66 (1992) 73–80.

[62] A.J. Sophianopoulos, C.K. Rhodes, K.E. Van Holde, The Journal of Biological Chemistry. 237 (1962) 1107–1112.

[63] F.Y. Lin, C.S. Chen, W.Y. Chen, S. Yamamoto, Journal of Chromatography A. 912 (2001) 281–9.

[64] A.J. Sophianopoulos, K.E. Van Holde, The Journal of Biological Chemistry. 239 (1964) 2616–2514.

[65] H. Larsericsdotter, S. Oscarsson, J. Buijs, Journal of Colloid and Interface Science. 289 (2005) 26–35.

[66] A. Kondo, K. Higashitani, Journal of Colloid and Interface Science. 150 (1992) 344–351.

[67] H. Huang, F. Lin, W. Chen, R. Ruaan, Journal of Colloid and Interface Science. 229 (2000) 600–606.

[68] F. Dismer, J. Hubbuch, Journal of Chromatography. A. 1149 (2007) 312–20.

[69] W.K. Chung, Y. Hou, A. Freed, M. Holstein, G.I. Makhatadze, S.M. Cramer, Biotechnology and Bioengineering. 102 (2009) 869–81.

[70] W.K. Chung, S.T. Evans, A.S. Freed, J.J. Keba, Z.C. Baer, K. Rege, et al., Langmuir : the ACS Journal of Surfaces and Colloids. 26 (2010) 759–68.